

AD-A236 812



RL-TR-91-63
Final Technical Report
June 1991



STUDIES OF OXIDE ANIONS

The Pennsylvania State University

A. Welford Castleman, Jr.

DTIC
ELECTE
JUN 13 1991
S E D

APPROVED FOR PUBLIC RELEASE; DISTRIBUTION UNLIMITED.

91-01982



Rome Laboratory
Air Force Systems Command
Griffiss Air Force Base, NY 13441-5700

91 6 12 061

This report has been reviewed by the Rome Laboratory Public Affairs Office (PA) and is releasable to the National Technical Information Service (NTIS). At NTIS it will be releasable to the general public, including foreign nations.

RL-TR-91-63 has been reviewed and is approved for publication.

APPROVED:



MARK K. HINDERS
Project Engineer

APPROVED:



JOHN K. SCHINDLER
Director of Electromagnetics

FOR THE COMMANDER:



IGOR G. PLONISCH
Directorate of Plans & Programs

If your address has changed or if you wish to be removed from the Rome Laboratory mailing list, or if the addressee is no longer employed by your organization, please notify RL(EECT) Hanscom AFB MA 01731-5000. This will assist us in maintaining a current mailing list.

Do not return copies of this report unless contractual obligations or notices on a specific document require that it be returned.

REPORT DOCUMENTATION PAGE

Form Approved
OMB No. 0704-0188

Public reporting burden for this collection of information is estimated to average 1 hour per response, including the time for reviewing instructions, searching existing data sources, gathering and maintaining the data needed, and completing and reviewing the collection of information. Send comments regarding this burden estimate or any other aspect of this collection of information, including suggestions for reducing this burden, to Washington Headquarters Services, Directorate for Information Operations and Reports, 1215 Jefferson Davis Highway, Suite 1204, Arlington, VA 22202-4302, and to the Office of Management and Budget, Paperwork Reduction Project (0704-0188), Washington, DC 20503.

1. AGENCY USE ONLY (Leave Blank)		2. REPORT DATE June 1991		3. REPORT TYPE AND DATES COVERED Final Jul 89 - Jun 90	
4. TITLE AND SUBTITLE STUDIES OF OXIDE ANIONS				5. FUNDING NUMBERS C - F30602-88-D-0028 Task - E-9-7147 PE - 63311F PR - 6331 TA - 00 WU - P4	
6. AUTHOR(S) A. Welford Castleman, Jr.					
7. PERFORMING ORGANIZATION NAME(S) AND ADDRESS(ES) The Pennsylvania State University Department of Chemistry 152 Davey Laboratory University Park PA 16802				8. PERFORMING ORGANIZATION REPORT NUMBER	
9. SPONSORING/MONITORING AGENCY NAME(S) AND ADDRESS(ES) Rome Laboratory (EECT) Hanscom AFB MA 01731-5000				10. SPONSORING/MONITORING AGENCY REPORT NUMBER RL-TR-91-63	
11. SUPPLEMENTARY NOTES Rome Laboratory Project Engineer: Mark K. Hinders/EECT/(617)377-4265					
12a. DISTRIBUTION/AVAILABILITY STATEMENT Approved for public release; distribution unlimited.				12b. DISTRIBUTION CODE	
13. ABSTRACT (Maximum 200 words) Several metal and metal oxide anion sources were used to investigate the formation and reactivity of species of relevance to the AFGL program. A new class of reactions were identified between anions of the form $H_xM_yO_z$, $1 \leq y \leq 2$; $1 \leq y \leq 5$; and $1 \leq z \leq 16$, for several metals including M=W, Ta, Ti, Mo, and HCl. The reactions have analogy to acid-base reactions. In another series of experiments, reactions of Al^- , and these clusters bound with V and or Nb, with O_2 were investigated. It was found that the Jellium model, though by no means a compendious concept, provides a good guide to the electronic structure of clusters and their general patterns of reactivity.					
14. SUBJECT TERMS Clusters, Reactions, Metal Oxide Anions				15. NUMBER OF PAGES 60	
				16. PRICE CODE	
17. SECURITY CLASSIFICATION OF REPORT UNCLASSIFIED	18. SECURITY CLASSIFICATION OF THIS PAGE UNCLASSIFIED	19. SECURITY CLASSIFICATION OF ABSTRACT UNCLASSIFIED	20. LIMITATION OF ABSTRACT SAR		

CONTENTS

Page

INTRODUCTION.	1
BRIEF OVERVIEW OF RECENT FINDINGS AND ACCOMPLISHMENTS	1
CONCLUSIONS	3
PUBLICATIONS.	4
PRESENTATIONS	4
APPENDIX A.	5
APPENDIX B.	8
APPENDIX C.	11
APPENDIX D.	43

Accession For	
NTIS GRA&I	<input checked="" type="checkbox"/>
DTIC TAB	<input checked="" type="checkbox"/>
Unannounced	<input type="checkbox"/>
Justification	
By _____	
Distribution/ _____	
Availability Codes _____	
Dist	Avail and/or Special
A-1	



INTRODUCTION

This contract dealing with reactions of metal oxide anion clusters commenced July 17, 1989. During the course of conducting work on the prior contracts, we developed several new ion-source techniques suitable for producing species of interest in the aforementioned context. One of them involves the utilization of a laser vaporization (LAVA) source, developed originally for the production of metal cluster anions comprised of aluminum and, more recently, extended to those of a wide variety of others including copper, titanium, vanadium, and niobium. As an alternative method we have been able to utilize a heated filament for producing metal oxide and metal hydroxide anions and related clusters of species including ones comprised of tungsten, tantalum, molybdenum and niobium. After demonstrating the feasibility of producing stable sources of the requisite anions by the above-mentioned methods, we undertook careful and detailed studies of their reaction mechanisms involving interaction with acid molecules, particularly HCl. Very rich and interesting acid-base reactions were identified, which represent very novel mechanisms heretofore not seen in the gas phase.

BRIEF OVERVIEW OF RECENT FINDINGS AND ACCOMPLISHMENTS

Using the filament source we were able to first produce tungsten oxide anions, reported earlier. The monomer, dimer, trimer, tetramer, and pentamer of WO_3^- were formed along with higher oxides of each species including WO_x^- , $x = 3, 4, 5$; W_2O_x^- , $x = 6, 7, 8, 9$; W_3O_x^- , $x = 9, 10, 11$; W_4O_x^- , $x = 12, 13$; W_5O_x^- , $x = 15$. WO_3^- was found to react with H_2O to form H_2WO_4^- while WO_4^- and WO_5^- were relatively unreactive. Thereafter, in a similar fashion, oxide anions of molybdenum, tantalum and niobium were produced. For the case of molybdenum, we observed oxides from MoO_3^- to $\text{Mo}_3\text{O}_{11}^-$, for tantalum, TaO_4^- to $\text{Ta}_5\text{O}_{16}^-$ and similar species for Nb.

Initial attention was focused on reactions of tungsten containing species, followed by studies of the reactions of tantalum and molybdenum oxide anions. The chemistry of reactions with HCl proved to be very complex, and considerable effort has been expended in unraveling the mechanisms. The recent results have yielded considerable insight into the nature of the species. The reactions of TaO_3^- , $\text{TaO}_2(\text{OH})_2^-$, and TaO_5^- with HCl were made for comparison with those for the corresponding niobium species, the latter of which was easier to analyze because of the single isotope of Nb. Analogous to the niobium case, all three tantalum oxide anions lead to the same four sequential products. The results show that whenever there is an OH unit bound to the metal oxide reactant, Cl from HCl replaces the OH unit which is then given off as H_2O . In the absence of OH units on the metal center, HCl adds in to form an OH group and a Cl bound to the metal atom. For $\text{MO}_2(\text{OH})_2^-$ (here M represents Ta or Nb) the sequence is: $\text{MO}_2(\text{OH})_2^-$, $\text{MO}_2(\text{OH})\text{Cl}^-$, MO_2Cl_2^- , $\text{MO}(\text{OH})\text{Cl}_3^-$, followed by MOCl_4^- . It is of interest to note that at about 0.3 torr He and $10 \text{ STP cm}^3 \text{ min}^{-1}$ HCl (0.001 torr HCl), for niobium the second and the fourth products ($\text{NbO}_2\text{Cl}_2^-$ and NbOCl_4^-) dominate, while for tantalum the third and fourth products dominate ($\text{TaO}(\text{OH})\text{Cl}_3^-$ and TaOCl_4^-). This suggests a difference between Ta and Nb for the conversion of MO_2Cl_2^- to $\text{MO}(\text{OH})\text{Cl}_3^-$ and that the tantalum species reacts faster at this step. The requirement here is that the metal center go from four coordinate (MO_2Cl_2^-) to five coordinate ($\text{MO}(\text{OH})\text{Cl}_3^-$). Tantalum and niobium are both group VB elements and this reactivity difference is almost certainly due to the additional electronic shell for tantalum.

Experiments were conducted for DCl reacting with the niobium oxides NbO_3^- and H_2NbO_4^- which facilitated efforts to identify the chemistry of the oxides and hydroxides. Both of these

oxides react with HCl to form $\text{NbO}_2(\text{OH})\text{Cl}^-$, or $\text{NbO}_2(\text{OH})_2^-$. Clearly NbO_3^- will react to give (after rearrangement) the deuterated species $\text{NbO}_2(\text{OD})\text{Cl}^-$. If H_2NbO_4^- is the hydrated species, $\text{NbO}_3 \cdot \text{H}_2\text{O}^-$, the product will be the same as for NbO_3^- , but if it has OH units attached to the central niobium metal atom then it will have the nondeuterated product $\text{NbO}_2(\text{OH})\text{Cl}^-$ at mass 177. The ratio of nondeuterated to deuterated product was such as to indicate that at least most of the H_2NbO_4^- is in fact $\text{NbO}_2(\text{OH})_2^-$. Titanium and vanadium negative oxides were also produced. These include VO_3^- , H_2VO_4^- , TiO_3^- , TiO_4^- , and H_2TiO_5^- . Reactions of these are currently under investigation.

Extensive effort has been devoted to studies of the reactions of aluminum anions with oxygen. Early studies from our group revealed very preferential reactions that seemed to well correlate with electronic shell closings based on a simple Jellium model. The results of oxidation experiments raised interesting questions about the very stable negative ion clusters which are produced as a result of oxidation reactions. In particular, it was found that Al_{13}^- and Al_{23}^- were produced at the expense of higher order clusters. These findings, which are reported in a paper referenced at the end of this document, fit reasonably well with the theoretical Jellium model. Reaction rate constants for the aluminum anions typically ranged from 7×10^{-13} to $7 \times 10^{-12} \text{ cm}^3/\text{sec}$, with the rates generally being slower for the even-electron species; the reactivities of Al_{13}^- and Al_{23}^- were found to be at least four orders of magnitude slower.

In order to further elucidate the factors governing the unusual stability of anion clusters, we initiated work on co-clustered species of aluminum with transition metals, in particular with niobium and vanadium. A new LAVA source technique was developed which enabled mixed clusters to be selectively obtained and studied, each containing one transition metal atom embedded/attached to the other anions. Following their introduction into the flow tube, O_2 was added through the reactant gas inlet and the reaction products monitored. As in the case of the bare aluminum anion systems, all of the clusters rapidly reacted forming stable clusters at the expense of the etching reaction. The most dramatic findings were the production of AlO_2^- , which was not observed as a product in the bare aluminum anion work. Additionally, in the case of niobium other prominent species which even dwarfed the Al_{13}^- (found to be the most stable species in prior oxidation work), were the formation of Al_4Nb^- and Al_6Nb^- . It is interesting to note that the Al_4Nb^- species is an 18-electron system, again being in accord with predictions of shell closings and non-reactivity based on the Jellium model. However, the Al_6Nb^- system deviates from these predictions. Further work with vanadium did not reveal the stable aluminum tetramer mixed cluster but did show the great stability of the Al_6V^- . These two findings differ substantially from predictions of the Jellium model and are leading us to new avenues of research to further elucidate the nature of these reactions.

An important question to which the present findings provide insight, concerns the counting of the d-electrons of transition metals in terms of the free electron model. In one version where the d-orbitals are considered to hybridize with the other orbitals in the cluster, all the valence electrons would participate in governing the electronic structure. In this case both vanadium and niobium would contribute five electrons to the cluster. Otherwise, the d-electrons would be considered as core electrons which would have V and Nb contribute 2 and 1 electrons, respectively. The observed odd-even alternation in reactivity is a clear indication that both atoms donate an odd number of electrons. The Jellium model accounts for the special stability of Al_{13}^- (and Al_{23}^-), and the stability of NbAl_4^- can also be explained by its electronic structure if all 5 electrons are available; this compound has 18 valence electrons which is a Jellium shell closing and also has special stabilities in coordination compounds (18 electron rule). If every valence electron is

counted as in the previous examples, VAl_6^- has 24 electrons which is not a predicted shell closing. (Note, however, if one of vanadium's electrons is promoted by hybridization, providing one free s-electron, the species then becomes a 20 electron system, and its lack of reactivity would be in accord with the Jellium model.)

CONCLUSIONS

In conclusion, the Jellium model is a good guide to the reactivity patterns and related electronic structure of metal alloy clusters, but by no means provides a compendious concept. The interaction of the electronic orbitals of aluminum with those of the transition metals may be sufficiently strong to enable all of the electrons to contribute to reactivity behavior as evidenced by the lack of differences for systems containing $4s^2$ and $5s^1$ electrons, and the general observation that odd-even electron number accounts for the reactivity of these alloy systems. Finally, it is interesting to speculate whether a structural form of VAl_5^- might not involve electron hybridization and hence would behave as an 18 electron system; this may account for the lack of reactivity of this species.

Some related work was also undertaken for aluminum cations for purposes of comparison to the anion work. Bi-molecular rate constants were measured for the disappearance of Al^+ through Al_{33}^+ . We did not see the anticipated slow rate for the reaction of Al_3^+ which would be expected to have a closed electronic shell and hence be comparatively unreactive. In the case of the cations, oxidation often leads to the retention of an oxide unit on the cation in contrast to the anion work. These findings lead to further questions concerning the overall generality of the Jellium model.

For more detailed information on the above-mentioned studies, please see Appendices A-D.

PUBLICATIONS

"Thermal Metal Cluster Anion Reactions: Behavior of Aluminum Clusters with Oxygen," R. E. Leuchtner, A. C. Harms, and A. W. Castleman, Jr., **J. Chem. Phys.** **91**, 2753 (1989).

"Gas Phase Reactivity of Metal Alloy Clusters," A. C. Harms, R. E. Leuchtner, S. W. Sigsworth and A. W. Castleman, Jr., **J. Am. Chem. Soc.**, in press.

"Aluminum Cluster Reactions," R. E. Leuchtner, A. C. Harms, and A. W. Castleman, Jr., **J. Chem. Phys.**, submitted.

PRESENTATIONS

"Reactions in Clusters: The Negative and Positive Aspects," invited Chemistry Departmental Seminar, University of Colorado, Boulder, October 9, 1989.

"Studies of the Chemistry of Radon Progeny Ions," invited talk, AAAR'89, Eighty Annual Meeting, Reno, Nevada, October 10-13, 1989.

"Photophysics of Clusters: Intracuster Reactions and Dynamics of Dissociation Processes," invited talk, Faraday Symposium 25 - Large Gas Phase Clusters, University of Warwick, London, December 12-14, 1989.

"Multiphoton Ionization of Clusters: Considerations of Dissociation Dynamics, Energy Release, and Bonding," 1989 International Chemical Congress of Pacific Basic Societies (PACIFICHEM), Honolulu, Hawaii, December 17-22, 1989.

"Clusters: Elucidating Solvation Effects on Reactins and Dissociation Dynamics," invited seminar, University of Pennsylvania, Philadelphia, PA, February 15, 1990.

"Studies of the Reactivity of Metal Cluster Ions Under Well-Defined Thermal Reaction Conditions," invited talk, ACS Symposium on Metal Clusters in Beams and on Supports: Chemistry and Catalysis, Boston, MA, April 23-27, 1990.

APPENDIX A

"Thermal Metal Cluster Anion Reactions: Behavior of Aluminum Clusters with Oxygen," R. E. Leuchtner, A. C. Harms, and A. W. Castleman, Jr., J. Chem. Phys. 91, 2753 (1989).

Thermal metal cluster anion reactions: Behavior of aluminum clusters with oxygen

R. E. Leuchtner, A. C. Harms, and A. W. Castleman, Jr.

Department of Chemistry, The Pennsylvania State University, University Park, PA 16802

(Received 7 April 1989; accepted 14 June 1989)

Investigation of the properties of metal clusters offers an excellent opportunity to study evolution of the solid state in a sequential, stepwise manner from the gas phase. In this communication we present what is, to the best of our knowledge, the first data on the reactivities of metal cluster anions equilibrated to a well-defined temperature in a flow tube. The aluminum anions (Al_n^- , $n = 5-40$) were produced by laser vaporization,^{1,2} thermalized in a high pressure flow tube (1.0 Torr) to room temperature and then allowed to react with oxygen. While the reactivities generally conform to predictions of the jellium model,³ there are some exceptions which probably are manifestations of local geometry.

Aluminum is appealing because in the solid state it is well represented by a free electron model, and with only three valence electrons per atom, it is readily amenable to theoretical treatment. In terms of the jellium model, a range of potential wells can be considered, two of which are the harmonic oscillator and Wood-Saxon. Hence, for aluminum anions, there are shell closings corresponding to $n = 13, 23$, and 37 (representing 40, 70, and 112 electrons) and $n = 11, 13, 19, 23, 35$, and 37 (representing 34, 40, 58, 70, 106, and 112 electrons) for the two different wells, respectively. We undertook a study of the anion reactivities under thermal conditions to test these predictions.

The apparatus employed presently has been used in our laboratory to study atomic ion reactions⁴; details of the laser vaporization (LAVA) source will be described elsewhere.⁵ Briefly, the aluminum target rod is vaporized by focussed 308 nm light in a 1.5 mm channel just upstream from a conical nozzle. The source is operated in a continuous rather than pulsed mode in order not to disturb the laminar flow of the system. The source pressure is typically 200 Torr and the buffer gas is helium. Cations and anions are formed in the

nozzle and no special secondary ionization is required. A well controlled concentration of oxygen is introduced into the flow tube downstream after the ablated material has undergone $\sim 10^5$ collisions.

Figure 1(a) shows the Al_n^- ($n = 5-24$) cluster distribution, calibrated using peak positions from tungsten oxide cluster anions.⁶ The average flow tube pressure was 0.95 torr, and the laser fluence was about 30 mJ/cm². The envelope of the distribution is similar to that of Gantefor *et al.*⁷ and represents a convolution of the neutral aluminum cluster abundances with the electron affinity of those species.

In Fig. 1(b), with 7.5 sccm of oxygen flowing, a dramatic loss of cluster signal is readily discerned for most species. However, Al_7^- , Al_{13}^- , Al_{15}^- , and Al_{17}^- have increased in intensity; evidently they are products of an etching reaction. It is important to note that $\text{Al}_{21}^- - \text{Al}_{23}^-$ have not diminished in intensity. An odd/even alternation, indicative of a paired electron effect, is evident where most of the even clusters have reacted away more so than the odd. The clear exception, Al_{22}^- , is surprising because all other even atom clusters are almost gone. The electron affinity of this species is anomalous,⁷ and likely has some special structural stability which makes it stable towards etching.

In Fig. 1(c), 100.0 sccm of oxygen has been added and we see that the most intense feature is clearly Al_{13}^- (its signal level has increased by a factor of 6). The peak at Al_{23}^- still persists, while Al_{22}^- has reacted almost completely away. Note that Al_{15}^- , Al_{16}^- , and Al_{17}^- also endure.

Due to lack of space, we have not displayed data taken in another mass range which shows the inertness of Al_{37}^- . While it is not produced by reaction of larger clusters, of which there are few, it is, however, unreactive over a wide oxygen concentration range. In general, our results appear to sup-

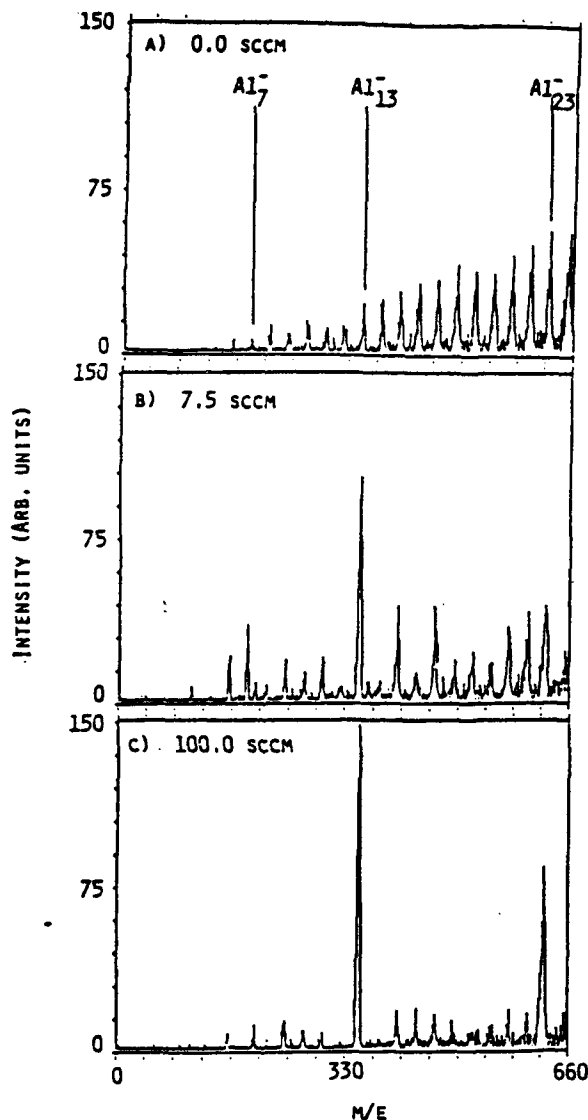


FIG. 1. Series of mass spectra showing progression of the etching reaction of aluminum anions (Al_7^- – Al_{24}^-) with oxygen. Note that these are all on the same intensity scale clearly showing production of Al_{13}^- and Al_{23}^- : (a) 0.0 sccm oxygen, (b) 7.5 sccm oxygen, (c) 100.0 sccm oxygen.

port the electron droplet (jellium³ model, although some anomalies, for example, the comparatively slow reactivities of $n = 7$ and 22, suggest that other effects, such as geometry,⁸ also contribute to the local behavior of some of the

clusters studied. It is interesting that the "magic" anion clusters fit better to jellium calculations using a harmonic oscillator potential in that they display inertness at $n = 13, 23$, and 37. By way of comparison to work on aluminum cations, some special abundances have also been seen that are in accord with considerations of electronic structure.⁹

Al_2O_2 and AlO_2 are the common products of two postulated etching reactions of the homologous anion series because they are exothermic,¹⁰ are gas phase products from alumina vaporization,¹¹ and are believed to be important in the oxidation of neutral aluminum clusters.¹²

We are continuing work with these small metal aggregates by quantitatively evaluating rate constants, as well as their reactivity toward other simple molecules. These results should aid in clarifying the accuracy of the simple unified atom picture of the jellium model.

Financial support by the Air Force Geophysics Laboratory, Contract No. RADCF30602-D-0025, is gratefully acknowledged.

¹T. G. Dietz, M. A. Duncan, D. E. Powers, and R. E. Smalley, *J. Chem. Phys.* **74**, 6511 (1981).

²V. E. Bondybey and J. H. English, *J. Chem. Phys.* **74**, 6878 (1981).

³(a) W. D. Knight, K. Clemenger, W. de Heer, W. Saunders, M. Chou, and M. Cohen, *Phys. Rev. Lett.* **52**, 2141 (1984); (b) M. Chou, A. Cleland, and M. Cohen, *Solid State Commun.* **52**, 645 (1984); (c) M. Chou and M. Cohen, *Phys. Lett. A* **113**, 420 (1986).

⁴A. W. Castleman, Jr., K. G. Weil, S. W. Sigsworth, R. E. Leuchtner, and R. G. Keese, *J. Chem. Phys.* **86**, 3829 (1987).

⁵R. E. Leuchtner, A. C. Harms, and A. W. Castleman, Jr. (to be published).

⁶R. E. Center, *Rev. Sci. Instrum.* **43**, 115 (1972).

⁷G. Gantefor, M. Gausa, K. H. Meiwes-Broer, and H. O. Lutz, *Z. Phys. D* **9**, 253 (1988).

⁸M. P. Iñiguez, M. J. Lopez, J. A. Alonso, and J. M. Soler, *Z. Phys. D* **11**, 163 (1989).

⁹(a) M. F. Jarrold and J. E. Bower, *J. Chem. Phys.* **85**, 5373 (1986); (b) **87**, 1610 (1987).

¹⁰(a) JANAF Thermochemical Tables, 3rd Edition, Part I, *J. Phys. Chem. Ref. Data* **14**, Suppl. 1 (1958); (b) The free energy of formation at 298 K for Al_2O_2 is -400 kJ/mol while for AlO_2 it is -91.7 kJ/mol.

¹¹(a) C. M. Fu and R. P. Burns, *High Temp. Sci.* **8**, 353 (1976); (b) P. Ho and R. P. Burns, *ibid.* **12**, 31 (1980).

¹²D. M. Cox, D. J. Trevor, R. L. Whetten, and A. Kaldor, *J. Phys. Chem.* **92**, 421 (1988).

APPENDIX B

"Gas Phase Reactivity of Metal Alloy Clusters," A. C. Harms, R. E. Leuchtner, S. W. Sigsworth and A. W. Castleman, Jr., **J. Am. Chem. Soc.** **112**, 5672 (1990).

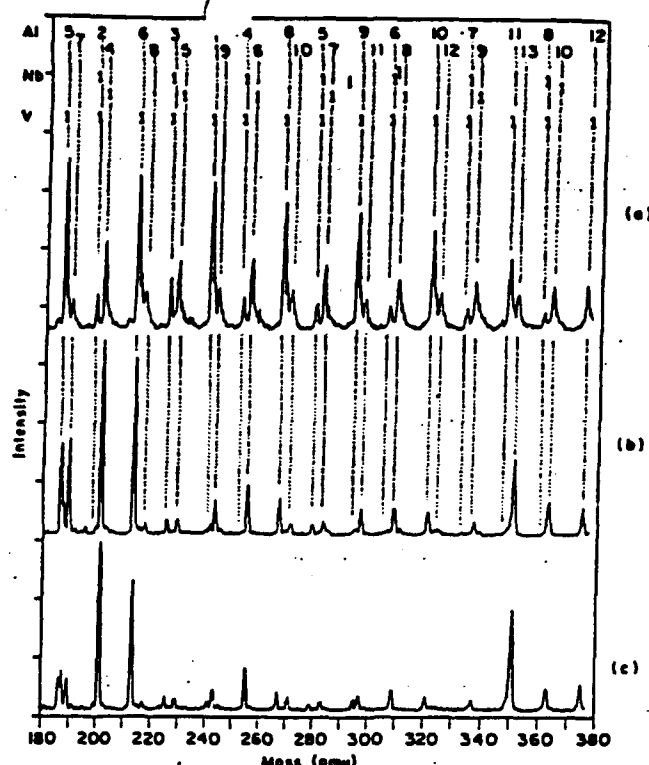


Figure 1. Reaction of metal clusters with O_2 : (a) 0.0 sccm of O_2 , (b) 30.6 sccm of O_2 , and (c) 60.0 sccm of O_2 . Intensity scales are arbitrary.

Gas-Phase Reactivity of Metal Alloy Clusters

A. C. Harms, R. E. Leuchtner, S. W. Sigsworth, and
A. W. Castleman, Jr.*

Department of Chemistry
The Pennsylvania State University
University Park, Pennsylvania 16802

Received March 26, 1990

Revised Manuscript Received May 21, 1990

Study of the production and reactivity of gas-phase mixed-metal clusters in a well-characterized flow reactor offers a unique opportunity to investigate the complex and interesting properties that often accompany the corresponding heterogeneous alloys. Determining the reactivity trends of small metal alloy particles provides a promising way not only of investigating the evolution of bulk behavior but also of elucidating the electronic and geometric makeup of metallic entities of finite dimensions. These latter aspects are currently the focus of intense experimental and theoretical activity.

The jellium model,¹ which treats the nuclei (and core electrons) of the constituent atoms as smeared out in a specified potential

well and allows all of the valence electrons of the cluster to fill electronic shells (as in the hydrogen atom), has been a useful model² in accounting for special abundances of small alkali clusters in terms of their electronic structure. In addition, recent results³ on the thermal reactivity (etching action) of bare aluminum cluster anions with oxygen showed Al_{13}^- and Al_{23}^- as products, species that are also predicted shell closings of the spherical jellium model.¹ However, the jellium model has failed to account for the trends in aluminum cluster polarizabilities⁴ and in some of their reactivity behavior.⁵ Moreover, magic numbers have been seen for cobalt clusters pointing to icosahedral structures,⁶ but none have been seen that can be attributed to the electronic structure of transition-metal clusters, raising questions about the general validity of the model.

One particularly useful way of investigating the importance of the electronic contribution to stability is by examining the influence of substituting one or more atoms in the cluster with one of differing valence.⁷ The present report deals with the reaction (etching action) of oxygen on aluminum clusters containing niobium and/or vanadium. Niobium and vanadium have five valence electrons each ($4d^45s^1$ and $3d^34s^2$, respectively), and aluminum has three ($3s^23p^1$). Determination of the trends in reactivity with cluster size, the produced magic number alloy clusters, and comparison of the results with the bare aluminum results sheds light on the jellium model, the importance of electronic effects, and the free electrons involved.

The details of the apparatus have been reported previously.⁸ The metal clusters are produced in a laser vaporization source

(2) Saito, Y.; Minami, K.; Ishida, T.; Noda, T. *Z. Phys. D* 1989, 11, 87.

(3) Leuchtner, R. E.; Harms, A. C.; Castleman, A. W., Jr. *J. Chem. Phys.* 1989, 91, 2753.

(4) de Heer, W.; Milani, P.; Châtelain, A. *Phys. Rev. Lett.* 1989, 63, 2834.

(5) (a) Leuchtner, R. E.; Harms, A. C.; Castleman, A. W., Jr. Aluminum Cluster Reactions, submitted. (b) Cox, D. M.; Trevor, D. J.; Whetten, R. L.; Kaldor, A. *J. Phys. Chem.* 1988, 92, 421.

(6) Klotz, T. D.; Winter, B. J.; Parks, E. K.; Riley, S. J. *J. Chem. Phys.* 1990, 92, 2110.

(7) Kappes, M. M. *Chem. Rev.* 1988, 88, 382.

(8) (a) Castleman, A. W.; Weil, K. G.; Sigsworth, S. W.; Leuchtner, R. E.; Kozee, R. G. *J. Chem. Phys.* 1987, 86, 3829. (b) Leuchtner, R. E.; Harms, A. C.; Castleman, A. W., Jr. Metal Cluster Cation Reactions: Carbon Monoxide Association to Cu_n^+ Ions. *J. Chem. Phys.*, in press.

(1) (a) Knight, W. D.; Clemenger, K.; de Heer, W.; Saunders, W.; Chou, M.; Cohen, M. *Phys. Rev. Lett.* 1984, 52, 2141. (b) Chou, M.; Cleland, A.; Cohen, M. *Solid State Commun.* 1984, 52, 645. (c) Chou, M.; Cohen, M. *Phys. Lett. A* 1986, 113, 420.

with continuous helium flow and thereafter introduced into a high-pressure flow-tube apparatus (ca. 0.5 Torr). The target rod is aluminum, and when the laser vaporization source is impregnated with niobium and vanadium, a distribution of bare aluminum and mixed-metal clusters is observed. The clusters are well thermalized before reacting with a neutral reagent (oxygen). Reactants and products are mass filtered and detected downstream with a quadrupole mass spectrometer and pulse counting techniques. Gases such as N_2 have been introduced without changing the original anion distribution, confirming the expected absence of collision induced dissociation processes in the flow-tube apparatus.

A portion of a typical spectrum is shown in Figure 1a. Several series of ions are seen, including the bare aluminum clusters Al_n^- ($n = 7-13$) and the mixed-metal clusters VAL_n^- ($n = 5-12$), $NbAl_n^-$ ($n = 4-10$), and $VNbAl_n^-$ ($n = 2-8$). The relative amounts of the mixed clusters compared with the bare aluminum clusters can be altered by changing the laser focus, and under certain conditions an additional series $V_2NbAl_n^-$ ($n = 0-6$) is also obtained in this mass range.

In Figure 1b, a spectrum covering the same mass range shows the results of the addition of 30.6 sccm of oxygen through the reactant gas inlet. The spectrum shows that nearly one-half of the peaks from the previous spectrum have reacted away. The reactivity pattern at this intermediate reaction condition evidently results from odd-even electron alternation and its concomitant influence on reactivity. With the exception of VAL_5^- , each of the remaining species in Figure 1b has an even number of electrons, indicating that the pairing of electrons increases the stability of the ions, or at least decreases their reactivities.

After the addition of 60.0 sccm of oxygen, three peaks dominate the spectrum. As can be seen in Figure 1c, these are Al_{13}^- , $NbAl_4^-$, and VAL_6^- . Al_{13}^- has been shown³ to be a stable product from the reaction of bare aluminum clusters with oxygen. In the current experiment the $NbAl_n^-$ clusters react to produce $NbAl_4^-$, and the VAL_n^- clusters react to produce VAL_6^- .

An important question to which the present findings provide insight concerns the counting of the d electrons of transition metals in terms of the free-electron model. In one version where the d orbitals are considered to hybridize with the other orbitals in the cluster, all the valence electrons would participate in governing the electronic structure. In this case both vanadium and niobium would contribute five electrons to the cluster. Otherwise, the d electrons would be considered as core electrons which would have V and Nb contribute two electrons and one electron, respectively.⁹ The observed odd-even alternation in reactivity is a clear indication that both atoms donate an odd number of electrons. The jellium model accounts for the special stability of Al_{13}^- (and Al_{23}^-), and the stability of $NbAl_4^-$ can also be explained by its electronic structure if all five electrons are available; this compound has 18 valence electrons, which is a jellium shell closing, and also has special stabilities in coordination compounds (18-electron rule). If every valence electron is counted as in the previous examples, VAL_6^- has 24 electrons, which is not a predicted shell closing. (Note, however, if one of vanadium's electrons is promoted by hybridization, providing one free s electron, the species then becomes a 20-electron system, and its lack of reactivity would be in accord with the jellium model.)

In conclusion, the jellium model is a good guide to the reactivity patterns and related electronic structure of metal alloy clusters, but by no means provides a compendious concept. The interaction of the electronic orbitals of aluminum with those of the transition metals may be sufficiently strong to enable all of the electrons to contribute to reactivity behavior, as evidenced by the lack of differences for systems containing $4s^2$ and $5s^1$ electrons and by the general observation that odd-even electron number accounts for the reactivity of these alloy systems. Finally, it is interesting to speculate whether a structural form of VAL_5^- might not involve

electron hybridization and hence would behave as an 18-electron system; this may account for the lack of reactivity of this species.

Acknowledgment. Financial support by the Air Force Geophysics Laboratory, Contract No. RADCF30602-88-D-0028, is gratefully acknowledged.

(9) (a) Ziman, J. M. *Principles of the Theory of Solids*; Cambridge Univ. Press: New York, 1972; p 113. (b) Cox, A. J. *Electronic Structure and Chemistry of Solids*; Oxford Univ. Press: Oxford, 1987; p 68.

APPENDIX C

"Aluminum Cluster Reactions," R. E. Leuchtner, A. C. Harms, and A. W. Castleman, Jr., J. Chem. Phys., submitted.

ALUMINUM CLUSTER REACTIONS

R. E. Leuchtner, A. C. Harms, and A. W. Castleman, Jr.

Department of Chemistry
The Pennsylvania State University
University Park, PA 16802

ABSTRACT

Aluminum clusters, both anion and cation, are produced using laser vaporization and reacted under thermal conditions with oxygen in a flow tube reactor. An etching reaction is observed and bimolecular rate constants are reported for Al_n^+ , $n=1-33$, and Al_n^- , $n=5-37$. For certain clusters, namely Al_7^+ , Al_{13}^- , and Al_{23}^- , no apparent reactivity is observed (they are found to be produced from larger species). Interestingly, these correspond to predicted jellium shell closings with 20, 40, and 70 electrons, respectively. Besides these exceptions, and a small odd/even alternation in reaction rates, the overall reactivity is relatively insensitive to cluster size, and is found to range between about 1×10^{-12} and $5 \times 10^{-12} \text{ cm}^3/\text{sec}$.

INTRODUCTION

The investigation of the properties of metal clusters under a variety of experimental conditions has provided a wealth of information concerning the evolution of the solid state with respect to that of the gas phase (1). With regard to the kinetics of reaction, there is a wide variability in reactivity as a function of the identity of the metal as well as cluster size; the explanation of these phenomena provide intriguing and exciting new challenges. Understanding how geometry and electronic structure affect reactivity can have tremendous impact on such diverse areas as thin film coating and catalysis (2).

The area of metal cluster chemistry is currently very active, prompted in part by the development of methods for producing these species in the gas phase. Specifically, laser vaporization (3,4) has become a very powerful technique for the ablation of refractory materials. The combination of laser vaporization followed by adiabatic expansion to produce small metallic and semi-metallic clusters has been coupled to many analytical techniques, for example, fast flow reactors (5), ion beam machines (6), and ion cyclotron resonance cells (7). Recently, this method of cluster production has been introduced onto a flow tube (8) operated under well defined thermal and flow dynamic conditions.

This report is a continuation of our previous communication concerning the reactivity of aluminum anion clusters with oxygen (9) (referred to hereafter as I), where the anomalous behavior was observed for several of the anions ($n = 13$ and 23), which correlated well with predictions of closed shell structures from the spherical jellium model (10). In the present study, laser vaporization was used to produce an ensemble of aluminum clusters, both anions and cations, which were then thermalized in a high pressure flow tube and subsequently allowed to react with oxygen (etching action). The initial ion distributions are presented, and lower limits to the bimolecular rate constants for the Al_n^- ($n = 5-37$), and Al_n^+ ($n = 1-33$) systems are given and discussed.

Aluminum is experimentally attractive because it has only three valence electrons per atom and is amenable to theoretical treatment. For metal clusters, especially transition metals, the density of states increases so rapidly that accurate molecular orbital calculations become impractical beyond aggregates with about ten atoms (11). For small clusters, the situation is still very complex. The choice of basis sets can have critical effects on the interpretation of bonding and geometry (12), and ground state assignments may sometimes be ambiguous. For example, there are at least six experimental and theoretical examinations of the lowest energy states of Al_2 (see, e.g., Ref. 12, and references therein) in which, depending upon the interpretation, lead to different conclusions.

On the other hand, the emergence of the electron droplet (jellium) model as a way of describing large metal aggregates has made approach to these systems theoretically tractable. For this approach, the electron-nuclear potential is approximated by a smooth, rounded well. Physically, the core electrons and nuclei of the metal particle are viewed as a conducting sphere. The delocalized valence electrons are allowed to fill orbital shells as if the cluster were a unified atom, and special stability is expected for those species that contain a full complement of electrons. Despite some failures in accounting for polarizability (13), this simple picture has worked remarkably well for describing magic numbers in the abundance spectra of the alkalis (13), steps or discontinuities in ionization potentials (14), as well as changes in the electron affinity of aluminum anions (15). As was shown in I, the electron droplet model can be used to explain many of the observed features regarding the etching action of oxygen upon aluminum. Reactivity is expected to be an important test of the shell closing model since a metal cluster's propensity to lose (or gain) electrons should be directly influenced by whether or not those electrons will leave an open or closed shell cluster after reaction. Special inertness toward reaction is expected for clusters with a full complement of electrons, while high reactivity should occur for clusters in which the product is a closed electronic system. In this regard, investigations pertaining to the influence of

charge on the observed reactivity should offer additional information as to the general validity of the shell model. The results of the present study serve to elaborate on the unusual reactivities of small metal aggregates, in general, as well as offer insight into the influence of geometric and electronic structure on reactivity.

EXPERIMENTAL

The flow tube and laser vaporization (LAVA) source have been described in detail elsewhere (8,9,16). Briefly, our LAVA source is similar in design to that of Dietz et al. (3) where the target material is vaporized in a channel just upstream from an expansion nozzle. Light (308 or 248 nm) from an excimer laser (Lambda Physik, model EMG 201 MSC) is focussed onto an aluminum rod with a twenty cm focal length quartz lens. A plasma is created inside a small (3 mm diam.) channel where a carrier gas (He, 99.995% Liquid Carbonic) transports the ablated material into a home-made brass nozzle. Critical to the production of clusters is a relatively high pressure in the vaporization region (~ 100-200 torr) as well as a finely polished exit cone on the nozzle. The source is operated in a continuous (17) rather than pulsed mode in order not to disturb the laminar flow of the subsequent flow reactor into which the clusters are injected for study.

The helium/plasma mixture expands into the flow tube (typically 0.25 - 1.3 torr) where adiabatic cooling occurs and supersaturation causes nucleation and growth of metal particles. Post ionization, e.g. dissociative attachment via an electron filament, is not necessary. Negative ions are most likely formed by electron attachment to pre-existing neutral clusters rather than nucleation around a negative ion core (see Ganteför et al. (15) and discussion below), while cations probably grow by sequential monomer additions to Al^+ .

Laminar flow is fully developed (Reynolds numbers ca. less than fifty) within 20 cm of the LAVA exit cone (18), and the reactant neutral is released into the flow about 30 cm downstream

from the source via a carefully designed inlet that minimizes entrance effects (19). The ion reaction time is accurately measured using pulsing techniques (16), and is typically between 5 - 15 milliseconds.

The detection region is a differentially pumped chamber where the pressure is usually less than 1×10^{-6} torr. A small amount of reactant and product ions are sampled on axis through a 1 mm sampling orifice. The sampled ions are mass selected by a quadrupole mass spectrometer, detected using a channeltron and analyzed using a pulse counting technique. The mass spectra are collected with a multichannel analyzer and are stored/analyzed using a personal computer.

RESULTS

1. Cluster Ion Production

Cations. Figure 1a shows a typical unreacted Al_n^+ ($n = 1-33$) cluster spectrum generated with the LAVA source. The laser wavelength was 248 nm and a fluence of about 30 mJ/cm^2 was used for all cation studies reported herein. The wavelength was changed to 308 nm and no significant change in the spectrum was observed. The average flow tube pressure was 0.29 torr and the flow rate of helium was 9000 standard cubic centimeters per minute (sccm).

Aluminum has a single observable isotope at 27 amu and a series of peaks corresponding to bare aluminum clusters are clearly visible for $n > 6$. Overall the spectrum is very similar to that reported by Jarrold and coworkers (20), where a rapid decrease of cluster intensity up to Al_4^+ followed by a broad larger cluster distribution, peaking around 3-400 amu, is observed. The hump that exists between about Al_7^+ and Al_{15}^+ is a background artifact (not present in the anion spectrum) and is presumably from the ionization and fragmentation of pump oil. The spectrum was taken at low resolution in order to enhance the cluster signal, a condition which contributes to the

broadness of this feature. It is observable even after the aluminum/oxygen reaction has gone to completion.

Between the bare clusters are seen aluminum oxide and/or water peaks. At low masses, many oxide impurities are evident, which tend to obscure the identification of the bare clusters (note the large Al_3O_3^+ peak). Typically, the Al_3^+ through Al_6^+ peaks are small in intensity. This, along with some unfortunate product interferences, makes rate evaluation for these species more difficult.

Of particular note is the lack of anomalous intensity breaks at the predicted jellium shell closings, Al_3^+ and Al_7^+ , for the cations (10c). In addition, the large break in the distribution at Al_{14}^+ , seen in many sputtered aluminum spectra (21,22), neutral aluminum mass spectra (23,24), and even cation spectra (20) produced by laser vaporization, is not observed. In all of these methods, however, loss of aluminum atom(s) follows ionization. It has been established by collision induced dissociation (CID) experiments (20) that the ionization potentials (IP's) of Al_2 through Al_{14} are greater than the monomer, while at Al_{15} , the IP drops below that of the atom. These facts have been used to argue for the unusual prominence of the Al_{14}^+ feature (20,21). Aluminum clusters grown by sequential atom condensation onto pre-existing cations, as is likely in the present case, would not be expected to display the Al_{14}^+ intensity aberration.

It is difficult in a few figures to fully illustrate the complex chemistry that is exhibited by the aluminum cluster/oxygen interaction. In Figure 1b is presented the aluminum cation distribution after reacting with 80.0 sccm of oxygen. First, a myriad of mixed oxides of several of the smaller aluminum cations are observed, e.g., AlO_x^+ , Al_2O_x^+ , and Al_3O_x^+ , where x ranges from 1 to 3 or 4. An abundant oxide, Al_5O_2^+ , was produced; an analogous product (with one more oxygen atom) has been seen in the case of the neutral cluster reactions (24), although in the case of the neutral species was much more prominent. Finally, some conspicuous oxides, whose intensities greatly depend on

source conditions, have been observed to be very intense (sometimes more so than the dimer, as in the present case); these include Al_3O_3^+ , AlO^+ and AlO_2^+ .

Anions. Figure 2 shows a typical aluminum anion spectrum generated with laser vaporization which displays a distribution of single peaks of negatively charged clusters up to Al_{40}^- . The laser wavelength was 308 nm (spectra using 248 nm were identical) and the fluence was less than 20 mJ/cm^2 . It should be noted that lower fluences are required to maximize the anion signal than for the case of the cation studies.

The spectrum was calibrated using peak positions from tungsten oxide anion clusters (25). The distribution extends higher, but the S/N ratio seriously degrades for masses beyond about Al_{40}^- for this instrument. Again, the scan was taken at low resolution (slightly higher than the cations) with peak widths about 5 amu wide. A small amount of the anions with a single oxygen atom attached is evident between each of the bare clusters. These are likely to result from an oxide impurity on the surface of the rod since their intensity does not correlate with subsequent oxidation reactions.

The mass spectral envelope is similar to the LAVA aluminum cluster anion spectrum of Ganteför et al. (15). The contrast in the intensity profiles (compare Figures 1a and 2) suggest that the anions are formed differently than the cations. There are no special features observed in the mass spectra and the anion distribution is probably a result of a convolution of the neutral aluminum cluster abundances and the electron affinity of those species.

In an attempt to test this, an electron emitting filament (26) was inserted into the flow tube, just downstream from the LAVA nozzle. It was found that the anion signal, on the average, increases by about twenty percent and that the general shape of the distributions envelope does not change dramatically. Since the number density of neutrals from the LAVA source greatly exceeds that of charged species (3), the signal increase observed must be due to the attachment of electrons

to neutrals. In addition, because cluster growth is effectively quenched upon exit from the LAVA nozzle and the distribution did not change, this suggests that the negative ion clusters from the LAVA source are likely formed by a similar process, i.e., electron attachment to pre-existing neutral species.

If a significant fraction of the cluster signal were due to condensation of metal atoms onto negative ions, special abundances of clusters like Al_{13}^- , would probably have been apparent in the initial unreacted distribution. However, it is possible that for relatively small neutral clusters, say $n < 7$, the attachment of the electron causes the evaporation of (an) atom(s), in order to become stable. This follows from the fact that Wöste et al. (27) observed fragmentation of small energized clusters, rather than autodetachment (except for Al_3^-).

Note that Al^- is not present even though it has a bound electron affinity (28) (the neutral monomer is probably the most plentiful species present in the plasma mixture after vaporization). This is probably due to the fact that the excess energy of electron attachment is inefficiently removed by collisions with helium and it simply autodetaches. The larger clusters, on the other hand, have more vibrational degrees of freedom in which the reaction energy may be statistically redistributed. From simple RRK theory (30), a geometrical increase in the metastable lifetime with the number of oscillators in the complex is expected. Therefore, although this unimolecular decay process will undoubtedly affect the entire shape of the anion distribution, the influence will be the greatest on the smaller clusters.

The expansion/vaporization conditions can be changed to enable a shift in the cluster distribution to higher or lower masses; however, the overall shape of the envelope remains similar with no distinct protuberances (as might be expected from the jellium model). This indicates that cluster formation is diffusion-limited where abundances are governed not by parent cluster binding energy, but by collisional growth with a constant sticking probability. Therefore, it was thought

that the reactivity of these anions rather than the simple interpretation of abundance spectra would provide more information on the general applicability of the jellium model.

In general, for the case of the anions, little or no oxides are observed as products (sometimes Al_7O^- is seen). This is in contrast to the case of the cations, where many oxide molecules are produced. As will be discussed below, the etching reaction removes atom(s) from the cluster and, depending on the sign, the charge resides with the species of lowest IP or highest electron affinity (EA).

In a related reaction, where NbAl_n^- species are etched by oxygen (31), both AlO^- and AlO_2^- are observed as products; ICR studies (32) of the aluminum anions have shown these anionic oxides, as well. The lack of observation of these oxides in the present study, is possibly due to autodetachment of the electron from the small oxide molecule.

As we reported previously (9), the dramatic growth of Al_{13}^- and Al_{23}^- , dominate the product spectrum. Upon reaction, these species, corresponding to 40 and 70 electron shell systems, increase rapidly in intensity and asymptote to a constant value.

2. Reactivity

Cations. The bimolecular rate constants for the disappearance of the $\text{Al}^+ - \text{Al}_{33}^+$ cation system are presented in Figure 3. The dotted line near the bottom of the figure roughly represents the theoretical measurement limit of the apparatus. By collecting mass spectra at 15 different oxygen concentrations in the flow tube, and obtaining the integral under each bare aluminum cluster mass in the $\text{Al}^+ - \text{Al}_{33}^+$ range, overall bimolecular rate constants were computed using the measured reaction time (4.69 msec) and a non-linear least squares method to fit the observed exponential decay. It should be noted that some species appeared to first, increase in intensity and then decay. The reported rates reflect a fit to only the decay portion of the intensity profile. For

Al_7^+ , the intensity is observed to increase throughout the entire 190 sccm oxygen (reactant) flow rate range employed.

For most of the clusters, the error in the rate is about 50% (error bars are shown for Al_{13}^+). For the clusters Al_4^+ - Al_8^+ , the production of oxide peaks as the reaction proceeded, represented a serious interference. While typical integration ranges were on the order of 3-4 amu, the rates reported for these species were obtained in a narrower range (< 1 amu). Nevertheless, because of possible mass interferences, they should be considered lower limits. In addition to the Al_7^+ peak, the Al_5^+ peak also increased in intensity, but then decreased. This could have been the result of the Al_3O_3^+ interfering in the pentamer integration region. Al_6^+ was not produced in the reaction, but its signal did not change; it is conceivable that Al_5O_2^+ caused some hindrance (167 amu) in observing intensity changes.

With respect to the reactivity pattern, the Al^+ and Al_7^+ species are not only unreactive, they are produced by the reaction(s). The monomer reaction is known to be endothermic with oxygen (34). The rate constant observed for the Al_3^+ cluster, which has been seen to be unreactive (34), is anomalous because it purportedly has a closed electronic shell (8 valence electrons). The rest of the clusters (except for Al_6^+ discussed earlier) exhibit decay rates (around $1\text{-}2 \times 10^{-12} \text{ cm}^3/\text{sec}$) with no overall trend in size. A small odd/even alternation in rate constants for Al_{18}^+ and above, whereby the even atom clusters exhibit higher reactivity, is thought to be a consequence of electron pairing. Finally a small dip in the reactivity plot is apparent around Al_{14}^+ and Al_{15}^+ .

Anions. In Figure 4, the effective bimolecular or overall disappearance rate for the anions as a function of cluster size is plotted. These data were obtained in a similar fashion as for the cations. In some cases (mostly the odd-atom clusters), e.g. Al_{15}^- and Al_{17}^- , the signal first increased before

decaying. In these instances, only the loss of signal and not the production part of the profile was modeled. The dotted line has the same significance as in Figure 3.

In order to demonstrate the shape of typical intensity profiles observed (representative of the cations, as well) the signal taken at 1.00 torr for Al_{14}^- and Al_{15}^- are plotted as a function of oxygen flow rate in Figure 5. The solid line represents the linear least squares fit as well as the data range modeled. Note the initial rapid decay (preceded by a rapid increase in signal for the Al_{15}^-) before the decay portion that is modeled. These features are reproducible and are greatly affected by flow tube pressure.

Non-zero rate constants are reported for Al_{13}^- and Al_{23}^- , even though they are produced in the reaction. This latter unreactivity appears to correlate well with almost complete depletion of the larger clusters; if these clusters react, then the rate constant is well below the measurement limit of the apparatus.

In general, like the cations, the rates of the other cluster sizes are relatively independent of size (about $1-5 \times 10^{-12} \text{ cm}^3/\text{sec}$). Beginning around Al_{11}^- or Al_{12}^- there is a distinct odd/even alternation in bimolecular rate constants, with the even atom clusters being more reactive than the odd for essentially the full mass range investigated. We pointed this fact out in our initial report (9); recent ICR spectra by Hettich (32) shows similar behavior.

Jarrold (35) has estimated the heat of oxygen chemisorption to be on the order of 10 eV, while Anderson and coworkers (36) have shown that the Al-Al binding energies for the small clusters ($n < 8$) are on the order of 1-2 eV. Given this order of exothermicity, a tremendous variety of reaction channels and energy disposal mechanisms exist.

In any formulation of the reactions that may occur with the aluminum clusters, account must be taken of the fact that the Al_{13}^- and Al_{23}^- are produced. This means that any reaction of the reactant aluminum cluster and the ensuing oxide that feeds these two product channels must leave

the charge on the bare aluminum cluster. Unfortunately, the knowledge of IP's and EA's on small gas phase aluminum oxides is limited. While many CID (35) results indicate that Al_2O is a major product from the oxidation of the cation clusters, this reaction would be unlikely to produce bare anions since it would involve two sequential losses of this molecule from the cluster, and we do not observe any significant amounts of (intermediate) suboxide products.

From our analysis, it is conjectured that AlO_2^- and AlO^- are likely products from the anion reactions (although probably not exclusively). Since no suboxide anions are observed, we speculate that another simple oxide, Al_2O_2 , could be formed. In the case of the anions, the following reactions should occur:



where the first reaction contributes to the production of the closed shell jellium clusters.

There is evidence that reaction (1) is reasonable. First, from the infrared spectroscopy of products of reactions of aluminum atoms in frozen matrices (38,39), and analysis of products evaporated from alumina (Al_2O_3) (40) in the presence of little or no oxygen, Al_2O_2 is found to be very abundant. Secondly, this reaction is consistent (without the charge) with data obtained for the neutral aluminum cluster reactions (23). In addition, if the exothermicity of reaction (1) is large, evaporation of atoms from the cluster anion could occur, as well. In the case of the anions, the

electron affinity of the clusters are all larger than the monomer (15), in which case evaporative loss would feed smaller anions.

While Reaction (2) is probably not highly exothermic (41), the $EA(AlO_2)$ is about 4 eV (42). This is higher than the reported electron affinity of the homogeneous aluminum clusters (15) and, therefore, the charge is expected to stay with the leaving oxide molecule and not with the cluster. Since this species is not observed as a product, it is possible that the oxide product is hot and the electron remains with the aluminum aggregate. It is surprising that the low pressure ICR studies (32) detected this species (as well as AlO^-), while we were unable to at higher pressures.

Speculating on the analogous reactions in the cation case is more difficult due to our inability to determine the parentage of the product oxides observed, i.e., from the existing suboxide impurities or from the bare clusters themselves. Since the IP's of the small oxides are much larger (the IP for AlO_2 (42), AlO (42), and Al_2O_2 (43), are 10.0, 9.5 and 9.9 eV, respectively) than the bare neutrals (20), reactions analogous to (1) and (2) will produce the bare cation clusters. The small drop in the rate constant near Al_{14}^+ (where the IP of the cluster becomes lower than the monomer) could be a manifestation of evaporative monomer loss as a result of the heat of reaction. It has also been shown (44) that the last two reactions (neglecting the charge) are exothermic for Al_3^+ and Al_4^+ , while reaction (1) was observed to be exoergic in the reaction of Al_2^+ .

DISCUSSION

1. Comparison of the Ions

It is interesting to compare some of the general features as well as the subtle features of the reactivity plots given in Figures 3 and 4, since it is expected that the chemistry for both types of ions is similar. The observed products should differ only by their relative ionization potentials (IP's) and electron affinities (EA's) compared to the respective charged cluster.

The single collision reactions of the aluminum cluster/oxygen system and CID studies of oxidized aluminum clusters show (35) a great propensity to lose one or more Al_2O units, but the present results do not bear this out. If Al_2O were produced in the anion reaction, at least some evidence of the corresponding suboxides, $\text{Al}_{n-2}\text{O}^-$, should have been found. In general for the anions, except for the one instance of Al_7O^- , no suboxide formation is observed in the present work.

The products from the cations are a large mixture of small suboxides and superoxides and include Al_2O^+ . Since the IP's of these oxides are quite large ($> 7 \text{ eV}$), these species probably result from reaction with existing metal oxide ions produced in the LAVA source.

As was pointed out above, the overall reactivity of the clusters is independent of the charge (about $1.5 \times 10^{-12} \text{ cm}^3/\text{sec}$). Since the clusters undergo a bimolecular reaction, a theoretical ion/molecule collision frequency may be computed from the Langevin expression (46). These rates depend slightly on the mass of the cluster, but range from 2.32×10^{-10} to $1.90 \times 10^{-10} \text{ cm}^3/\text{sec}$ over the Al to Al_{40} range. These are roughly two orders of magnitude larger than the experimentally observed rates.

At a median flow rate of 100 sccm, an average pressure of about 0.3 torr, and a reaction time of 5 milliseconds, the aluminum clusters will collide with an oxygen molecule roughly one hundred times; of these, only one or two will go on to form products. In some of the intensity profiles (especially for the anions), a rapid increase in signal followed by a much slower decay was observed. While only the decay portion of the profile was modeled, the signal increase is obviously due to a cascade from larger clusters.

Several groups studying the aluminum cation system have reported activation barriers to oxygen chemisorption (37,47). The breaking of an oxygen bond (about 5 eV) and the formation of an Al-O bond has been estimated to be about 7.5 eV(35). While this large amount of energy will likely fragment the smaller clusters, even under the relatively high pressures presently employed,

the activation process might involve electron donation into an anti-bonding orbital of the oxygen molecule. This can be used to explain some of the irregularities in the observed reactivity patterns.

In the case of the odd/even alternation, electron donation from a cluster which has an unpaired electron will probably be more facile than for the case where no unpaired electrons exist. For the cations, where there is less electron density in general, the pairing effect is much less pronounced (the rates ranging from about $1-2 \times 10^{-12}$ cm³/sec versus $1-5 \times 10^{-12}$ cm³/sec) compared to the anions.

Clearly the most striking feature of the reaction profiles are not only the unreactivity, but the formation of certain clusters predicted to be stable from the spherical jellium model, namely Al_7^+ , Al_{13}^- , and Al_{23}^- , which are 20, 40, and 70 electron systems, respectively. Their unreactivity is also explainable in light of the above mentioned oxygen/aluminum cluster interaction, but more dramatically because the electronic shell closing represents a change in stability of the cluster with respect to its neighbors.

It is interesting to look more closely at the predictions of the shell model and the general influence of electronic structure on reactivity. If the jellium representation of metal clusters is accurate, then those clusters that have a closed shell should also demonstrate special stability with regards to their inertness to reaction. We find that this is generally the case for the aluminum ions, where these special species are not only unreactive but are also produced from larger clusters.

Some would argue that there are shells which do not show any special stability, for example, the shell closings at Al_{11}^- and Al_{19}^- , as well as Al_3^+ . There appear to be reasonable explanations however, for their behavior.

The reactivity of Al_3^+ was, at first surprising, because it has been reported to be unreactive by Anderson et al. (34) under single collision conditions. Furthermore, it represents an important shell closing with 8 valence electrons. The shell model appears to break down for small metal

clusters especially those with more than one valence electron. This can be explained in light of the fact that a smooth spherical potential is not really an accurate representation of a small cluster with only several atoms. It has been pointed out by Upton (48) that significant electronic perturbations in these small systems caused by strong ionic core potentials and high point group symmetries may cause changes in the observed shell filling order.

Along these same lines, the choice of the proper nuclear potential well in describing the various shells is important as well, since the degeneracies of many of the closings are removed upon the use of Wood-Saxon potentials compared to the harmonic oscillator well. It can be said that, for aluminum, the shell closings appear to occur for a system modeled using the harmonic oscillator. Wöste (27) has pointed out, as have Chou and Cohen (10c), that the strength of the aluminum bond compared to other single electron systems is large, making the potential less square compared to, say sodium. In the case of Al_{11}^- and Al_{19}^- (34 and 58 electrons, respectively), it may be possible that 1f and 1g shells are more reactive.

Qualitatively, it appears as if the anions might demonstrate the jellium influence more clearly than the cations. This may be a manifestation of special spatial geometries of the 13 and 23 atom clusters. Al_{13} has been studied theoretically (49) and has been calculated to have D_{3h} symmetry like an hcp metal. On the basis of this structural information alone, one might suspect that this species would be less reactive than its neighbors.

The cluster, Al_{13}^- , has a complement of 40 electrons. Jellium calculations on neutral aluminum (10c) indicate that shell closings are smeared out over several clusters and the abruptness is not sharp as in the single electron systems. This appears to be inconsistent with our findings, since unreactivity is located at single-sized clusters and not over a range of species.

Recently, Iniquez et al. (50) have had success in the application of density functional theory in concert with the jellium model to predict electronic and geometric properties of small metal

clusters. For aluminum, they found that Al_{13} represents the first species that has a complete geometric shell around a central atom (an icosahedron with an atom at the center), while Al_{23} is the first species that has a complete shell with two atoms at the center. In an indirect way, the effects of such structural irregularities like dangling bonds could make a particular cluster more reactive. In such a situation, the enhanced stabilities of these two anions could be a combination of both electronic and structural factors.

2. Comparison with Bulk Aluminum

The behavior of the aluminum ions in general are remarkably similar; this is in contrast to the case of the relative neutral rate constants reported by Cox et al. (23) where a maximum in the reactivity plot is observed at Al_2 , followed by a rapid decay in the rate constant, a minimum at Al_4 and Al_7 , and then a gradual rise in reactivity towards the level of the dimer out to Al_{30} . The reaction for the case of the neutrals was postulated to be different from that reported in cation CID studies (36,37). The most abundant product observed was Al_3O_2 , and it was thought to be formed as the result of further reaction of Al and an aluminum monomer or dimer with an oxygen molecule chemisorbed onto it.

A substantial activation barrier has been reported (37,47) for the breaking of the oxygen molecule. There is still some controversy as to whether a molecularly chemisorbed state exist on a bulk aluminum surface for oxygen(51); however, a larger amount of data suggests that oxygen dissociatively chemisorbs even at low temperatures (52), indicating no barrier. For the clusters, the fact that a highly exothermic process does not proceed at the collisional rate implies that either a barrier to dissociation exists or that some particular molecular orientation of the reacting pairs is required. While it can be argued that the reactions observed on aluminum surfaces are quite

different from those occurring on the aluminum clusters, both must involve an initial attack by the oxygen molecule.

The small sticking coefficients of oxygen onto a variety of different crystal faces of aluminum (from 0.04 on the Al(110) and Al(111) faces to 0.008 on Al(001), could imply that the dissociation requires surfaces steps, kinks, etc. in order to occur (51). For the case of the aluminum clusters, it may be argued that many high index "crystal faces" are open to attack by the incoming oxygen molecule, i.e., the surface atoms will be packed in such a way that they act like the surface defects required for dissociation.

From the theory of chemisorption (53), the observed sticking coefficient is related linearly to an orientation factor (called the condensation coefficient) and exponentially to an activation barrier,

$$s = \sigma f(\phi) e^{-E/RT} \quad (4)$$

where s is the sticking coefficient, σ is the condensation (probability) coefficient, $f(\phi)$ ($= 1$ presently) is a function of the surface coverage, T is the temperature, R the gas constant, and E is the activation energy. If we assume that the condensation coefficient is unity, then, in the low coverage limit (initial oxygen attack), the sticking coefficient can be directly equated to the activation barrier of the reaction.

The sticking coefficient for the clusters can be obtained from the ratio of the observed rate constant to the theoretical collision frequency. Presently, this corresponds roughly to 0.005 to 0.008, and represents an activation energy of around 0.12 to 0.14 eV at room temperature (E for the anions is slightly smaller than for the cations). This is much smaller than the value of 0.55 eV reported by Jarrold and Bower (47) and is intermediate to the range of values reported by Anderson et al. (37).

While the thresholds for activation reported by these researchers vary dramatically with cluster size, the error bars associated with these values are quite large. The presently computed value seems reasonable and appears to explain the general reactivity for those species that do react. Since the computed activation barrier is relatively independent of cluster size, it is interesting, in light of these conjectures, how the transition from an activated chemisorption to a non-activated, surface specific, dissociative chemisorption will occur.

CONCLUSIONS

The bimolecular rate constants for the overall disappearance of small (< 40) aluminum clusters (both positive and negative) are reported. The reactivity profiles show a general overall independence of charge and cluster size. Three reactions were postulated to occur that help explain the observed reaction products (or lack thereof), but given the large exothermicities likely involved in the general oxidation of aluminum, other reaction channels probably arise as well.

Cluster reactivity differences were observed which were easily explainable within the proposed oxygen/cluster ion reaction mechanism. An odd/even alternation was apparent for both anions and cations, where the odd atom species were less reactive than the even numbered neighbors.

Special unreactivity was found for those clusters corresponding to closed electronic shells (Al_{13}^- , Al_{23}^- , and Al_7^+). Indeed, these ions were actually produced in large quantities from the etching action of oxygen upon larger clusters. The distinct unreactivity of these particles with regard to charge and size, strongly suggests the importance of electronic structure in explaining their stabilities, and hence how the observed ion profiles changed as the reaction proceeded. Geometry probably also lends somewhat to the stability of these clusters (especially the anions), since the 13 and 23 atom cluster corresponds to geometric shell closings, as well.

The overall reactivity of the aluminum clusters were described in terms of an activated chemisorption. While the sticking coefficients of the clusters and bulk aluminum are of similar magnitude, the behavior in each case results from different phenomena. For surfaces, the oxygen is dissociatively chemisorbed and the low sticking probability is related to the condensation coefficient (a particular surface defect is probably required). For the clusters, the interaction involves an initial chemisorbed state with a condensation coefficient which is likely to be near unity, and subsequent reaction involves surmounting an activation barrier (ca. 0.12-0.14 eV).

ACKNOWLEDGMENTS

Financial support by the U.S. Department of Energy, Grant No. DE-FGO2-88-ER60668, and the Air Force Geophysics Laboratory, Contract No. RADCF30602-88-D-0028, is gratefully acknowledged.

REFERENCES

1. F. Trager and G. zu. Putlitz, ed., "Metal Clusters", Springer, Heidelberg, 1986.
2. (a) M.D. Morse, Chem. Rev. 86, 1049 (1986); (b) A.W. Castleman, Jr. and R.G. Keesee, Chem. Rev. 86, 589 (1986).
3. Dietz, M.A. Duncan, D.E. Powers and R.E. Smalley, J. Chem. Phys., 74, 6511 (1981).
4. V.E. Bondeybey and J.H. English, J. Chem. Phys. 74, 6878 (1981).
5. (a) S.J. Riley, E.K. Parks, G.C. Nieman, L.G. Pobo and S. Wexler, J. Chem. Phys. 80, 1360 (1984); (b) M.E. Geusic, M.D. Morse and R.E. Smalley, ibid 83, 2293 (1985).
6. P. Fayet and L. Woeste, Surf. Sci. 156, 134 (1985)
7. (a) S.W. McElvany, W.R. Creasy, and A. O'Keefe, J. Chem. Phys. 86, 715 (1987); (b) W.D. Reents, A.M. Muijsce, V.E. Bondeybey and M.L. Mandich, ibid 86, 5568 (1987).
8. R.E. Leuchtner, A.C. Harms, A.W. Castleman Jr. J. Chem. Phys. 92, 6527 (1990).
9. R.E. Leuchtner, A.C. Harms, A.W. Castleman, Jr., J. Chem. Phys. 91, 2753 (1989).
10. (a) W.D. Knight, K. Clemenger, W. de Heer, W. Saunders, M. Chou, M. Cohen, Phys. Rev. Lett. 52, 2141, (1984); (b) M. Chou, A. Cleland, M. Cohen, Solid State Commun. 52, 645 (1984); (c) M. Chou and M. Cohen, Phys. Lett. 113A, 420 (1986).
11. F. Casula, W. Andreoni, K. Maschke, J. Phys. C 19, 5155 (1986).
12. C.W. Bauschlicher Jr., H. Partridge, S.R. Langhoff, J. Chem. Phys. 86, 7007 (1987).
13. Y. Saito, K. Minami, T. Ishida and T. Noda, Z. Phys. D 11, 87 (1989).
14. W.A. Saunders, K. Clemenger, W.A. de Heer, W.D. Knight, Phys. Rev. B 32, 1366 (1985)
15. G. Gantefoer, M. Gausa, K.H. Meiwes-Broer and H.O. Lutz, Z. Phys. D 9, 253 (1988).
16. A. W. Castleman Jr., K.G. Weil, S.W. Sigsworth, R.E. Leuchtner and R.G. Keesee, J. Chem. Phys. 86, 3829 (1987).
17. S.C. Richtsmeier, E.K. Parks, K. Liu, L.G. Pobo and S.J. Riley, J. Chem. Phys. 82, 3659 (1985).
18. Dushman, S. and Lafferty, J.M., "Scientific Foundation of Vacuum Technique", 2nd. Wiley, New York, (1962).

19. B.L. Upschulte, R.J. Shul, R. Passarella, R.G. Keesee and A.W. Castleman Jr., *Int. J. Mass Spectrom. Ion Proc.* **75**, 27 (1987).
20. M.F. Jarrold, J.E. Bower, and J.S. Kraus, *J. Chem. Phys.* **86**, 3876 (1987).
21. F.L. King and M.M. Ross, *Chem. Phys. Lett.* **164**, 131 (1989).
22. R.F.K. Herzog, W.P. Poschenrieder, and F.G. Satkiewicz, *Radiation Effects* **18**, 199 (1973).
23. D.M. Cox, D.J. Trevor, R.L. Whetten, and A. Kaldor, *J. Phys. Chem.* **92**, 421 (1988).
24. K. Fuke, S. Nonose, N. Kikuchi, and K. Kaya, *Chem. Phys. Lett.* **147**, 479 (1988).
25. R.E. Center, *Rev. Sci. Instr.* **43**, 115 (1972).
26. D. Macnair, *Rev. Sci. Instr.* **38**, 124 (1967).
27. W.A. Saunders, P. Fayet, and L. Wöste, *Phys. Rev. A*, **39**, 4400 (1989).
28. C.S. Fiegerle, R.R. Corderman and W.C. Lineberger, *J. Chem. Phys.* **74**, 1513 (1981).
29. M. Meot-Ner, in "Gas Phase Ion Chemistry", edited by M.T. Bowers (Academic, New York, 1979), Vol. 1, p. 197.
30. J. Bernholc and J.C. Phillips, *Phys. Rev. B* **33**, 7395 (1986).
31. A. C. Harms, R. E. Leuchtner, S. W. Sigsworth and A. W. Castleman, Jr., *J. Am. Chem. Soc.* **112**, 5672 (1990).
32. R.L. Hettich, *J. Am. Chem. Soc.* **111**, 3582 (1989).
33. P.R. Bevington, "Data Reduction and Error Analysis for the Physical Sciences", McGraw-Hill, 1969, Chap. 11.
34. L. Hanley and S. Anderson, *Chem. Phys. Lett.* **129**, 429 (1986).
35. M.F. Jarrold and J.E. Bower, *J. Chem. Phys.* **87**, 5728 (1987).
36. L. Hanley, S.A. Ruatta, and S.L. Anderson, *J. Chem. Phys.* **87**, 260 (1987).
37. S.A. Ruatta, L. Hanley, and S.L. Anderson, *Chem. Phys. Lett.* **137**, 5 (1987).
38. L.V. Serebrennikov and A.A. Mal'tsev, *Vest. Mosk. Khimiya (ser.2)* **40**(2), 137 (1985).
39. S.M. Sonchik, L. Andrews and K.D. Carlson, *J. Phys. Chem.* **87**, 2004 (1983).
40. R.H. Lamoreaux, D.L. Hildenbrand and L. Brewer, *J. Phys. Chem. Ref. Data*, **16**(3), 419 (1987).

41. Since $\text{WH}_f(\text{AlO}_2) = -20.6 \text{ kcal/mole}^{42}$ and an Al-Al bond is on the order of 25-75 kcal/mole^{32,37} compared to the aluminum atomization energy of 82 kcal/mole⁴², this means approximately 25-75 kcal/mole will be released in the reaction.
42. M.W. Chase, Jr., C.A. Davies, J.R. Downey, Jr., D.J. Frurip, R.A. McDonald, and A.W. Syverud, "JANAF Thermochemical Tables", 3rd Edition, Part I, J. Phys. Chem. Ref. Data 14, Suppl. 1 (1985).
43. O.E. Kashinenov, A.D. Chervonyi, and V.A. Piven, High Temp. Sci. 15, 79 (1982).
44. S.A. Ruatta and S.L. Anderson, J. Chem. Phys. 89, 273 (1988).
45. D.L. Hildenbrand, Chem. Phys. Lett. 20, 127 (1973).
46. G. Giourmoussis and D.P. Stevenson, J. Chem. Phys. 29, 294 (1958).
47. M.F. Jarrold and J.E. Bower, J. Am. Chem. Soc. 110, 6706 (1988).
48. (a) T.H. Upton, Phys. Rev. Lett. 56, 2168 (1986); (b) T.H. Upton, J. Chem. Phys. 86, 7054 (1987).
49. H. Partridge, C.W. Bauschlicher, Jr., J. Chem. Phys. 84, 6507 (1986).
50. M.P. Iniquez, M.J. Lopez, J.A. Alonso, and J.M. Soler, Z. Phys. D 11, 163 (1989).
51. I.P. Batra and L. Kleinman, J. Electron Spectrosc. Relat. Phenom. 29, 225 (1983).
52. J.E. Crowell, J.G. Chen, and J.T. Yates, Surf. Sci. 165, 37 (1986).
53. See, for example, D.O. Howard and B.M. Trapnell, "Chemisorption", 2nd ed., Butterworths, Washington, D.C., 1964, Chapter III.
54. The condensation coefficient must be > 0.01 since reaction occurs at least once in every 100 collisions.

FIGURE CAPTIONS

Figure 1. (a) Spectrum of aluminum cations, Al_n^+ , ($n=1-33$). (b) Spectrum of aluminum cations, Al_n^+ with 80.0 sccm of oxygen.

Figure 2. Spectrum of aluminum anions, Al_n^- , ($n= 5-40$).

Figure 3. Bimolecular rate constants versus cluster size for the Al_n^+ /oxygen system.

Figure 4. Bimolecular rate constants versus cluster size for the Al_n^- /oxygen system.

Figure 5. (a) Intensity profile of Al_{14}^- versus oxygen addition (1.00 torr). (b) Intensity profile of Al_{15}^- versus oxygen addition (1.00 torr).

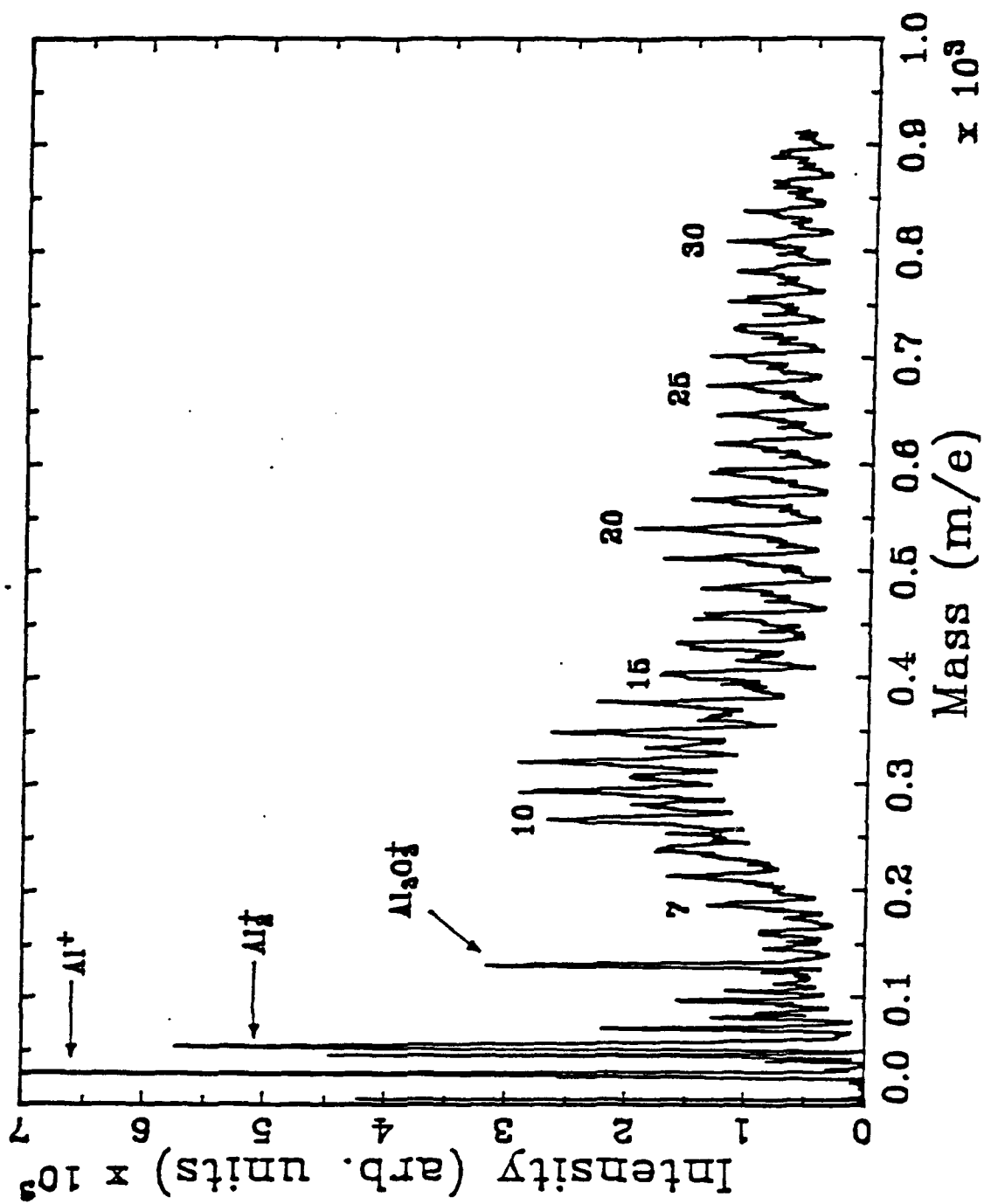


Figure 1(a)

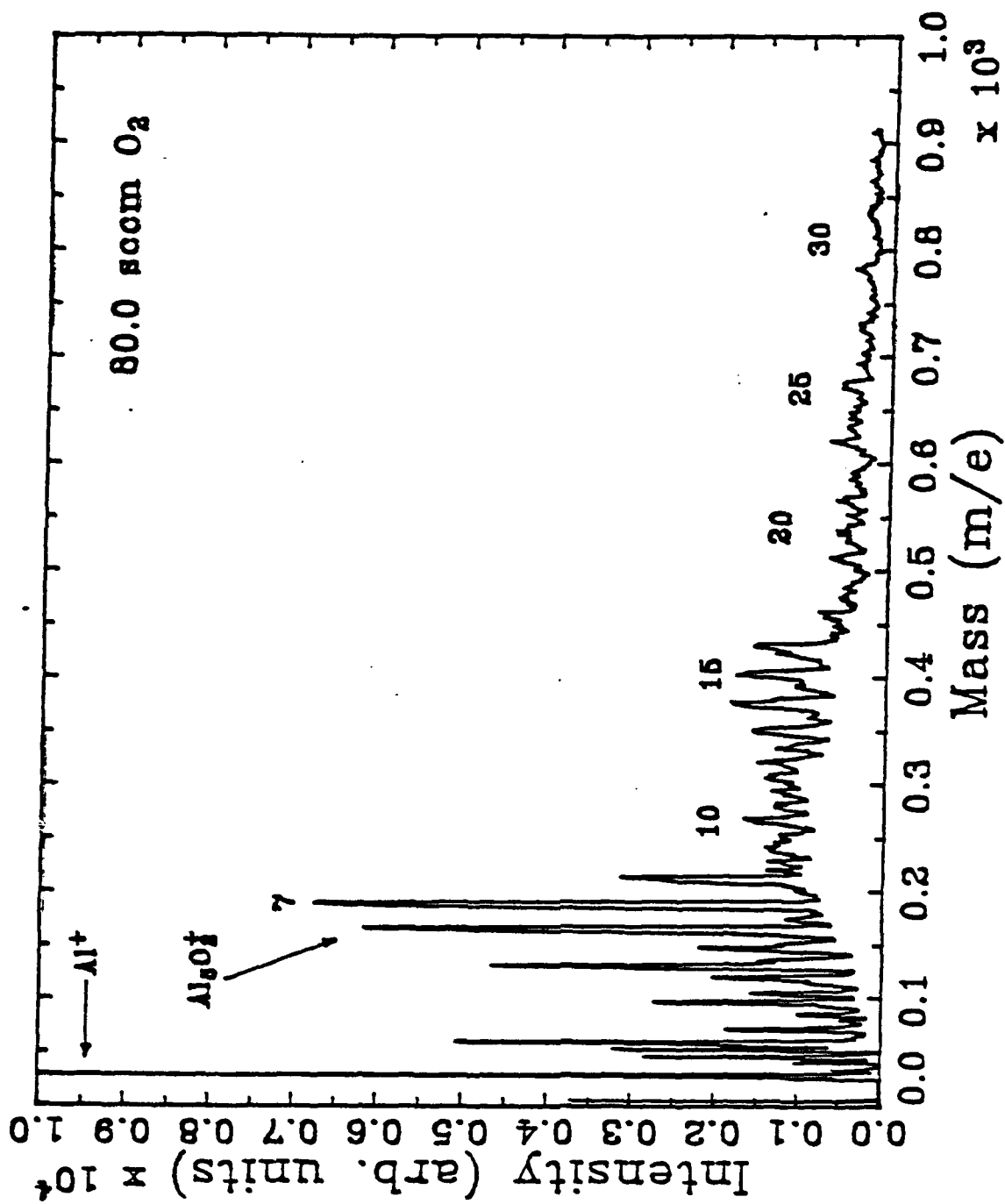


Figure 1(b)

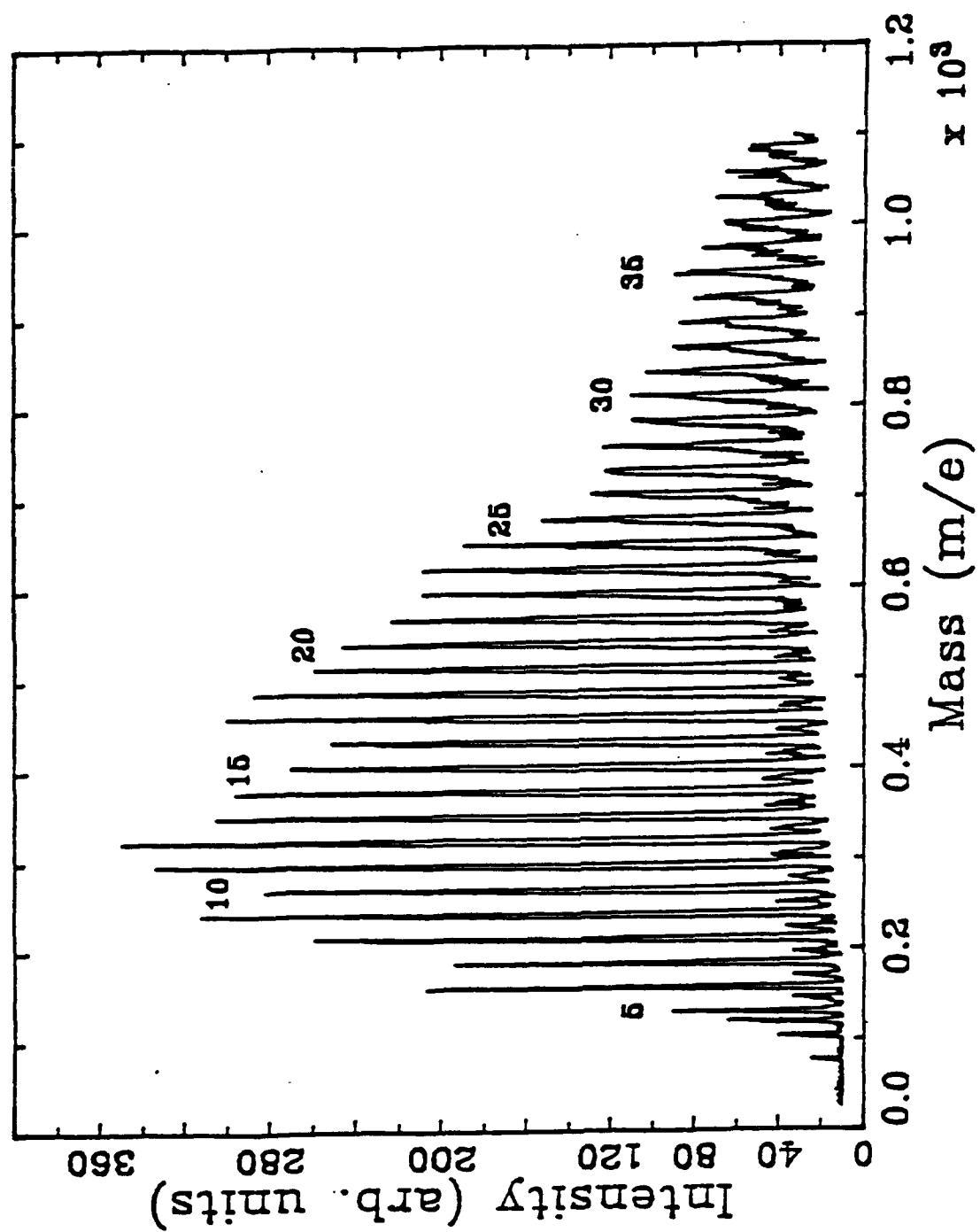


Figure 2

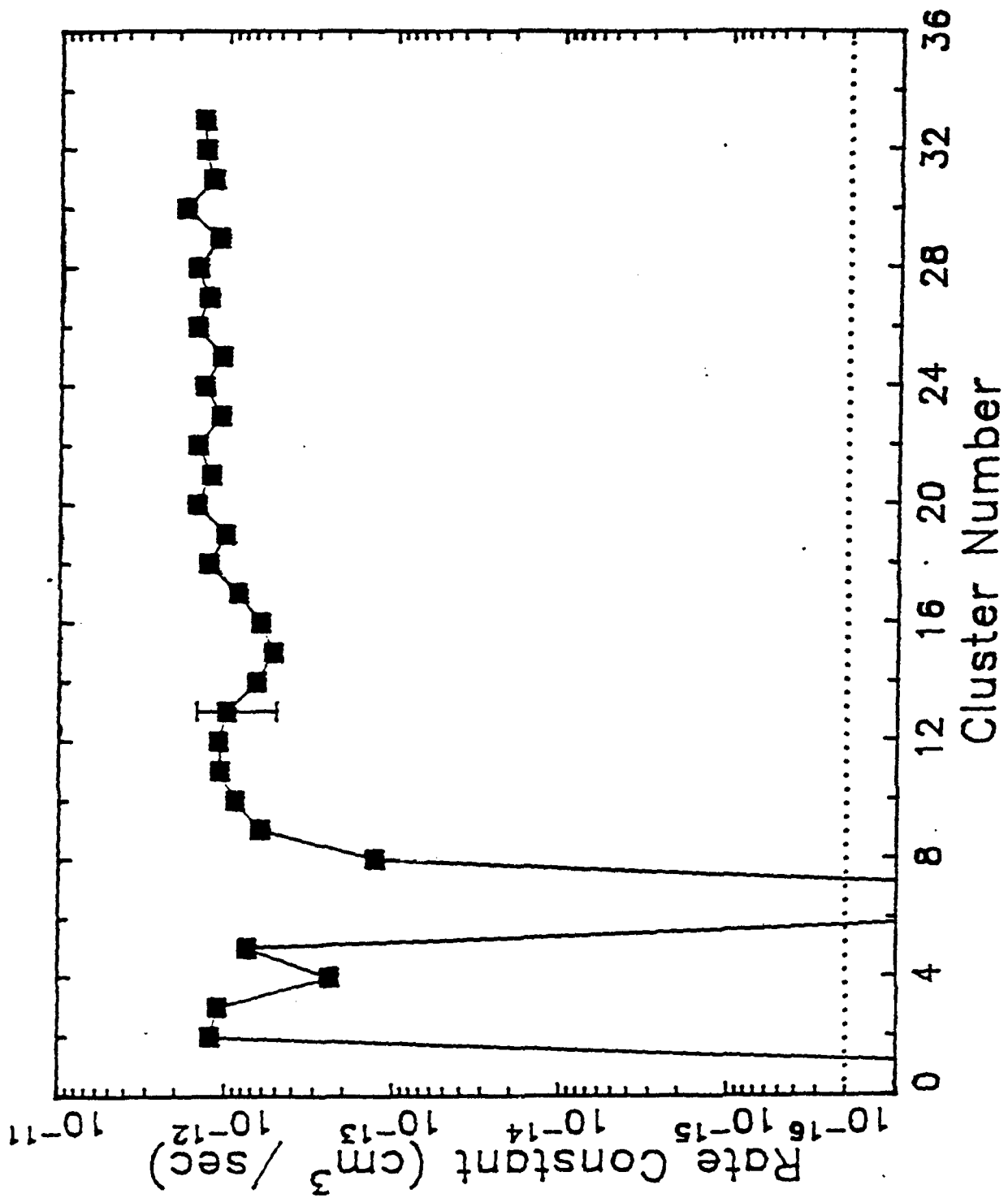


Figure 3

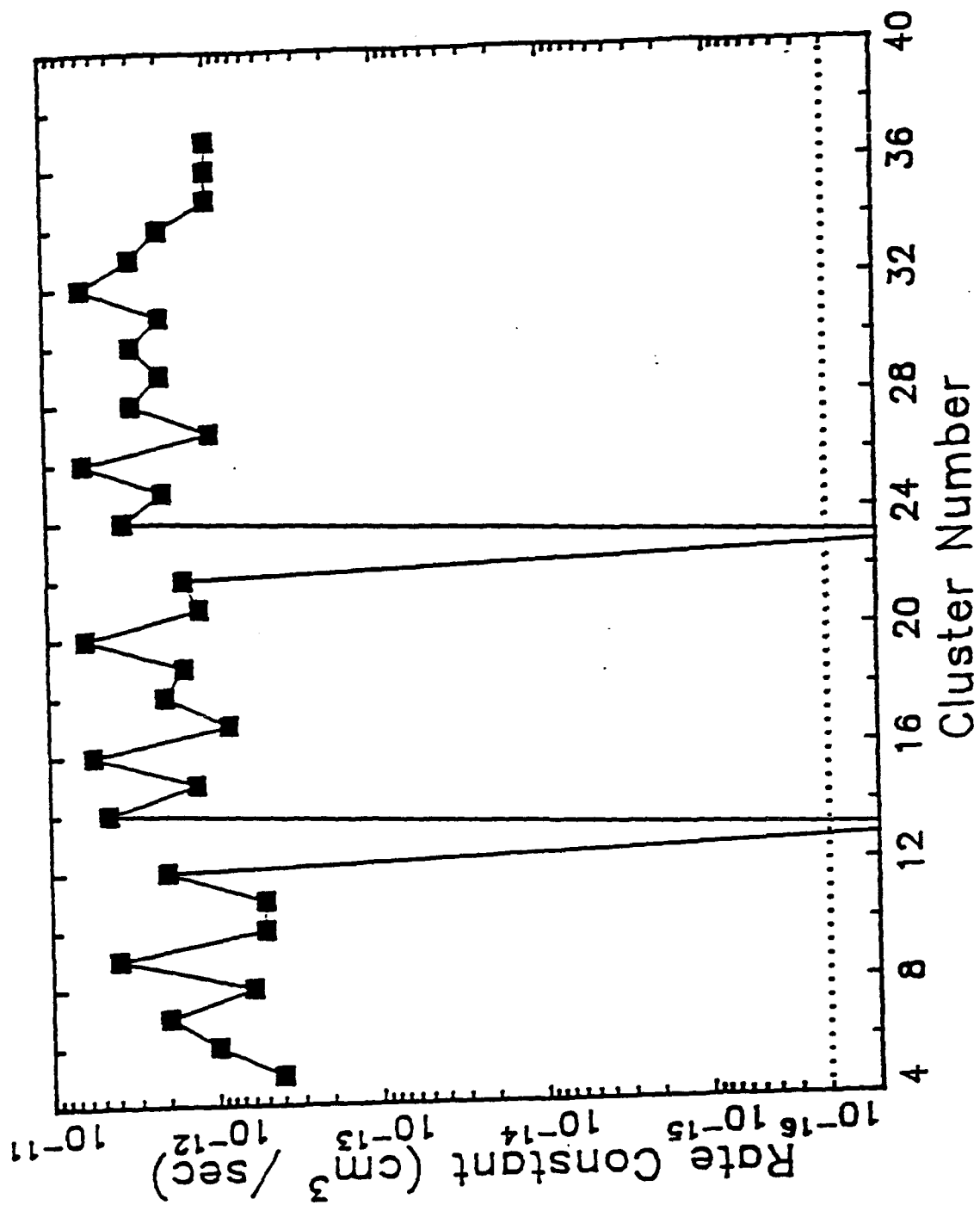


Figure 4

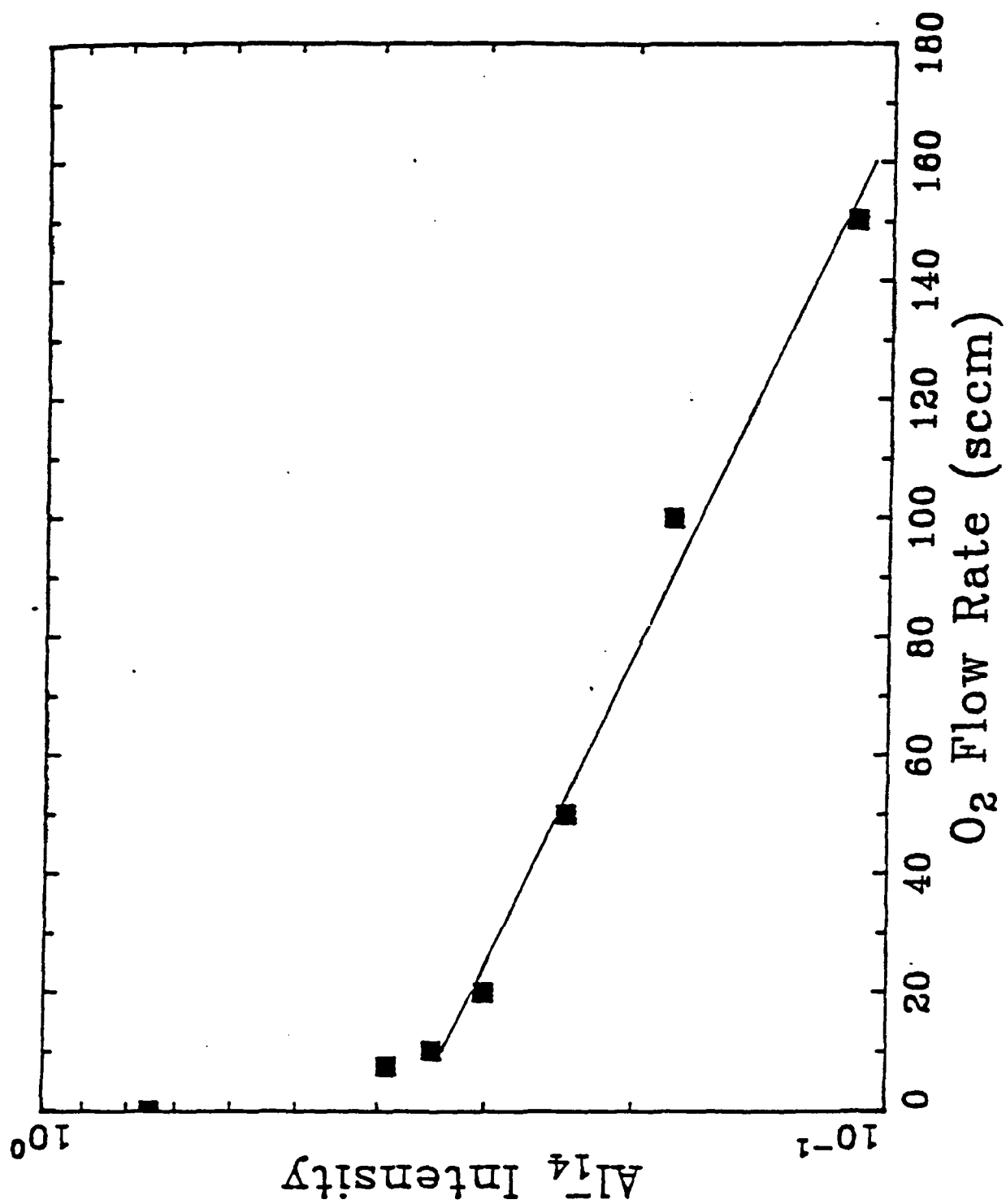


Figure 5(a)

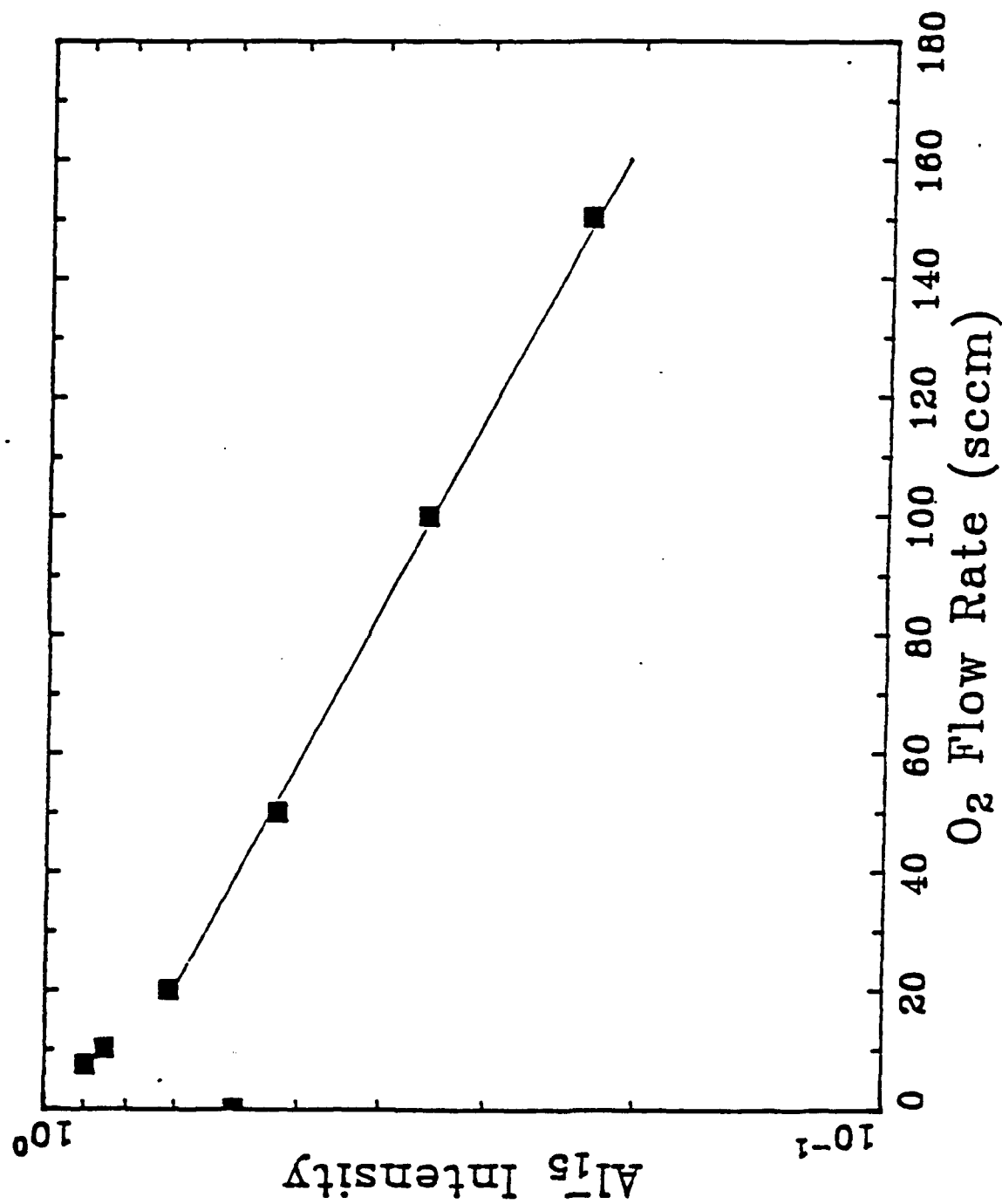


Figure 5(b)

APPENDIX D

"Gas Phase Acid-Base Neutralization Reactions: Niobium Oxide Anions with HCl," S. W. Sigsworth and A. W. Castleman, Jr., in preparation.

**Gas Phase Acid-Base Neutralization Reactions:
Niobium Oxide Anions with HCl**

S. W. Sigsworth and A. W. Castleman, Jr.

Department of Chemistry
The Pennsylvania State University
University Park, PA 16802

ABSTRACT

Novel reactions are observed for niobium oxide anions. The anions NbO_3^- , H_2NbO_4^- , and NbO_5^- undergo reactions with HCl that appear to be of acid-base type; for whenever hydrogens are present on the anion, Cl from HCl replaces an OH unit on the metal center giving H_2O as the neutral product. Moreover, whenever no hydrogens are present on the anion, HCl adds in to form an OH unit and a Cl unit bonded to the niobium center. After four sequential additions of HCl, all three ionic reactants lead to the final product NbOCl_4^- .

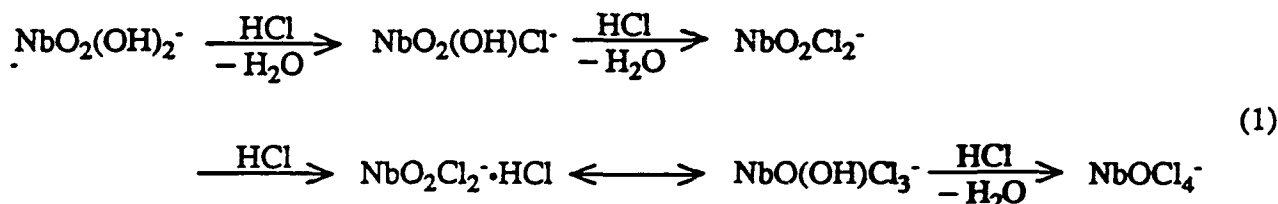
Currently, there is extensive interest in the chemistry of metal oxides, molecular aggregates, and nanosized particles and their anions (1). Molecules of the oxides are formed in oxidation reactions, and nanosized particles and thin films play a role in a wide variety of applied areas from catalysis to microelectronics (2). Furthermore, metal oxide species usually have high electron affinities and are important as electron scavengers in high temperature combustion and related oxidation reactions. We report herein observations of novel reactions of various niobium oxide anions with HCl, which bear analogy to acid-base interactions.

The reactions were observed at room temperature in a flow-tube apparatus described previously (3). Ions are produced by a technique in which a small flow of O₂ is added to 150 STP cm³ s⁻¹ He flow and passed over an incandescent niobium filament, biased at ca. 200 volts. Niobium oxides are thereupon emitted from the surface as anions. These reactant ions are thermalized by means of large numbers of collisions with the He buffer gas and then are allowed to react with HCl added downstream. Reactant and product ions are detected in the usual manner with a quadrupole and a particle multiplier set up for pulse counting. The He and O₂ used are of high purity (99.995 and 99.99%, respectively) and the He was further purified by passage through molecular sieve traps. Nevertheless, sufficient water was still present to enable the formation of hydrated niobium oxide species.

The reactant ions of interest are NbO₃⁻, H₂NbO₄⁻ and NbO₅⁻, simultaneously present in the flow tube (see Figure 1a). These anion reactions appear to be of an acid-base type; for whenever hydrogens are present on the anion, Cl from HCl replaces an OH unit on the metal center giving H₂O as the neutral product. Also, whenever there are no hydrogens initially present on the anion, HCl adds on to form an OH unit and a Cl unit each bonded to the Nb center. As before (3), although the molecular formula for each ionic species is determined from its mass and isotopic distribution in the mass spectrum, the isomeric arrangement of atoms is revealed from an observation of the reactions that occur. This crucial latter point is further discussed in what

follows. After sufficient HCl is added the final product is NbOCl_4^- , a well-known stable anion in solution phase chemistry (4). All three reactant ions have the same ionic products and their reactions differ only in the formation of initial non-ionic products. For NbO_3^- there is no neutral product for the first reaction step, while H_2NbO_4^- and NbO_5^- give off H_2O and O_2 , respectively, in their initial reaction with HCl.

The species H_2NbO_4^- may be represented as $\text{NbO}_3^- \cdot \text{H}_2\text{O} \longleftrightarrow \text{NbO}_2(\text{OH})_2^-$. Assuming this to be true, conversion from a hydrated ion to one with two hydroxyl groups should be easily accomplished through a hydrogen bonding interaction, given that the oxygen atom of the water molecules is datively coordinated to the niobium atom. Thereby, the anion $\text{NbO}_2(\text{OH})_2^-$ should be then convertible to NbOCl_4^- through four sequential additions of HCl and the loss of three H_2O molecules.

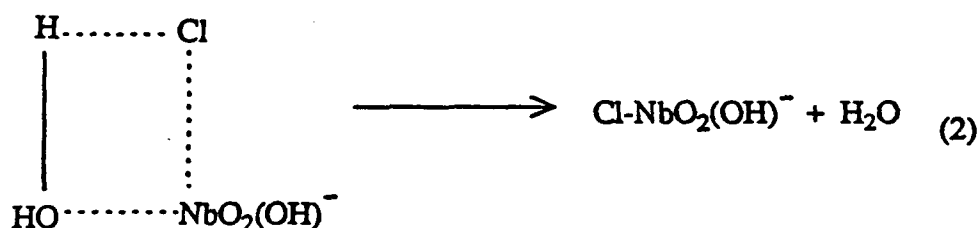


In Figure 1a, the initial reactants NbO_3^- , H_2NbO_4^- and NbO_5^- appear at masses 141, 159 and 173 amu, respectively. It is easy to see from Figures 1b and 1c, that the initial product at 177 and 179 amu, $\text{NbO}_2(\text{OH})\text{Cl}^-$, reacts with HCl to form $\text{NbO}_2\text{Cl}_2^-$ at 195, 197 and 199 amu. The third and fourth products, $\text{NbO}(\text{OH})\text{Cl}_3^-$ and NbOCl_4^- show up as clusters of peaks beginning at 231 and 249 amu, respectively.

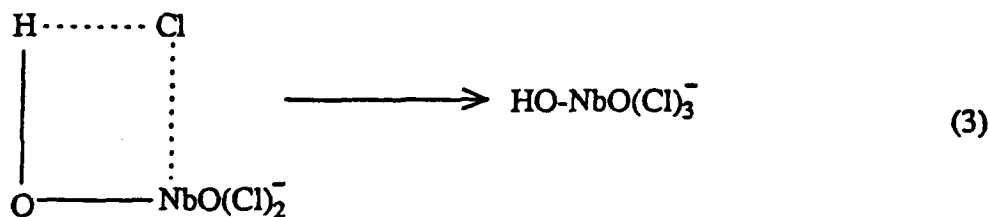
Brief studies were conducted with deuterium chloride to ascertain the nature of H_2NbO_4^- . Such studies are complicated by the fact that NbO_3^- , NbO_5^- , and H_2NbO_4^- are simultaneously present and all have the same initial ionic product, $\text{NbO}_2(\text{OH})\text{Cl}^-$, though they differ in the initial neutral product. With NbO_3^- and NbO_5^- , the initial product should be deuterated, $\text{NbO}_2(\text{OD})\text{Cl}^-$,

since no hydrogens are donated to a neutral product from the reaction pair. For H_2NbO_4^- , the initial product would be deuterated if H_2NbO_4^- is $\text{NbO}_3^-\cdot\text{H}_2\text{O}$ (switching to form $\text{NbO}_3^-\cdot\text{DCl}$) and nondeuterated if it is $\text{NbO}_2(\text{OH})_2^-$ (reaction forms $\text{NbO}_2(\text{OH})\text{Cl}^- + \text{HDO}$). The ratio of nondeuterated to deuterated initial product was such as to indicate (within experimental error) that H_2NbO_4^- is in fact $\text{NbO}_2(\text{OH})_2^-$.

When HCl interacts with $\text{NbO}_2(\text{OH})_2^-$ and forms a successful reaction pair, the reaction could conceivably proceed either by H attack at the oxygen of an OH unit or by Cl attack at the niobium metal center. Initial attack by Cl would require that HCl acts as a base and the metal oxide anion as an acid, but this seems unlikely. For HCl acting as an acid, the reaction should proceed through an intermediate as follows:



This mechanistic step is repeated one more time for $\text{Cl-NbO}_2(\text{OH})^-$ to give $\text{NbO}_2\text{Cl}_2^-$ and H_2O . For $\text{NbO}_2\text{Cl}_2^-$ reacting with HCl , the reaction can be envisioned to proceed as follows after initial attack by the hydrogen of HCl :



The $\text{HO-NbO}(\text{Cl})_3^-$ is then ready to give off H_2O when it reacts with HCl to form NbOCl_4^- in a manner analogous to Equation (2).

Interestingly, these reactions of metal oxide anions follows a very simple mechanism which bears a direct analogy to condensed phase acid-base reactions.

Acknowledgments:

Financial support by the Air Force Geophysics Laboratory, Contract No. RADC-F30602-88-D-0028, is gratefully acknowledged.

References

1. (a) A. W. Castleman, Jr. and R. G. Keesee, *Science* **241**, 36 (1988); (b) A. W. Castleman, Jr. and R. G. Keesee, *Ann. Rev. Phys. Chem.* **37**, 525 (1986); (c) A. W. Castleman, Jr. and R. G. Keesee, *Chem. Rev.* **86**, 589 (1986).
2. R. P. Andres, et al., *J. Mater. Res.* **4**, 704 (1989).
3. (a) A. W. Castleman, Jr., K. G. Weil, S. W. Sigsworth, R. E. Leuchtner, and R. G. Keesee, *J. Chem. Phys.* **86**, 3829 (1987); (b) S. W. Sigsworth, R. G. Keesee, and A. W. Castleman, Jr., *J. Am. Chem. Soc.* **110**, 6682 (1988); (c) S. W. Sigsworth and A. W. Castleman, Jr., *J. Am. Chem. Soc.* **111**, 3566 (1989); (d) S. W. Sigsworth and A. W. Castleman, Jr., *Chem. Phys. Lett.* **168**, 314 (1990).
4. F. A. Cotton and G. Wilkinson, *Advanced Inorganic Chemistry*, 4th ed. (Wiley-Interscience, New York, 1980).

Figure Caption

Figure 1. At 9000 sccm or 0.32 torr helium, HCl is added to a distribution of NbO_3^- , H_2NbO_4^- and NbO_5^- at mass flow rates of (a) 0.0, (b) 1.0, (c) 6.1 and (d) 20.4 sccm. The initial product for all three initial anionic reactants is $\text{NbO}_2(\text{OH})\text{Cl}^-$ at 177 and 179 amu. Thereafter, sequential products show up as a triplet, a quartet and a quintet of peaks beginning at 195, 231 and 249 amu, corresponding to $\text{NbO}_2\text{Cl}_2^-$, $\text{NbO}(\text{OH})\text{Cl}_3^-$ and NbOCl_4^- , respectively.

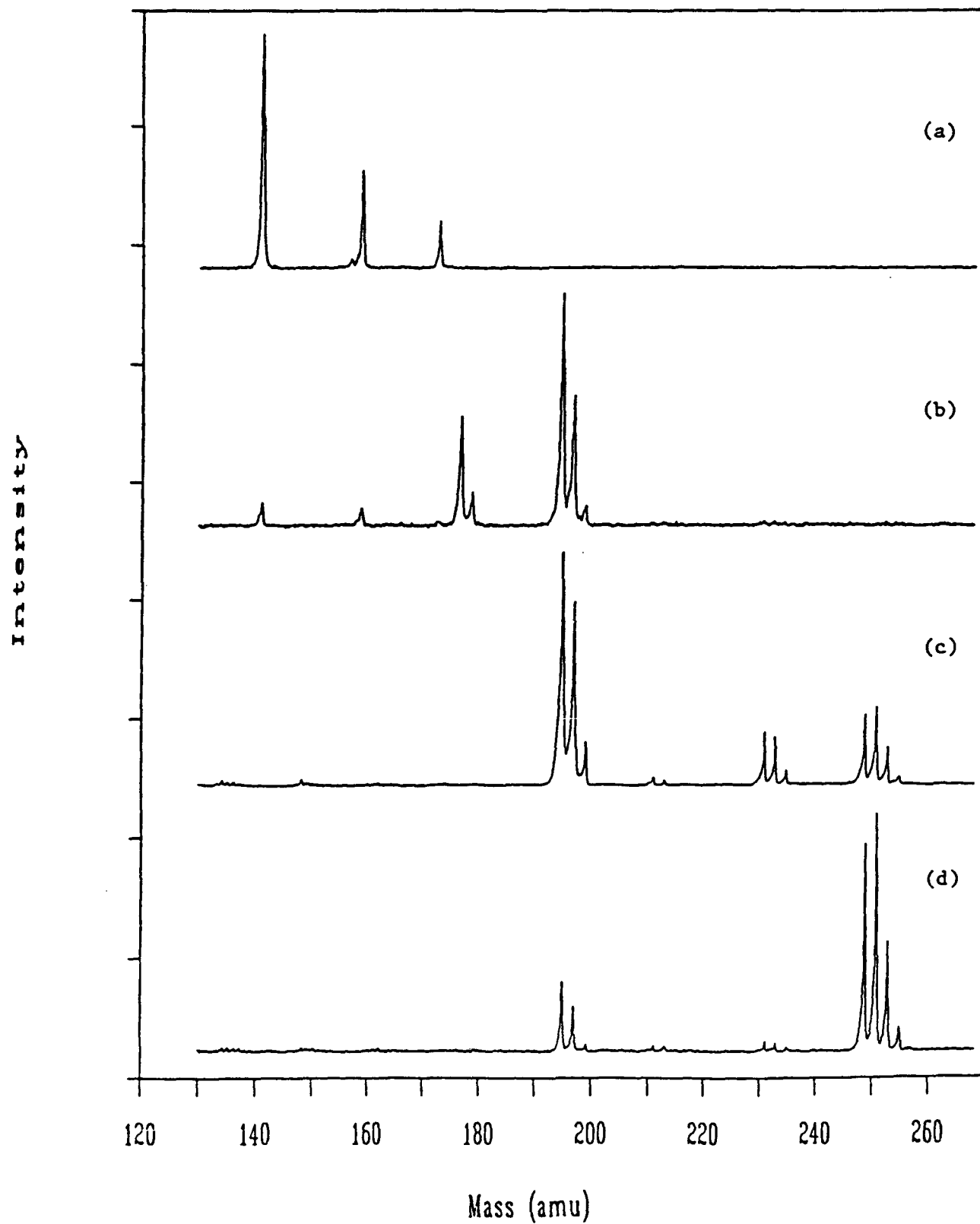


Figure 1

**MISSION
OF
ROME LABORATORY**

Rome Laboratory plans and executes an interdisciplinary program in research, development, test, and technology transition in support of Air Force Command, Control, Communications and Intelligence (C³I) activities for all Air Force platforms. It also executes selected acquisition programs in several areas of expertise. Technical and engineering support within areas of competence is provided to ESD Program Offices (POs) and other ESD elements to perform effective acquisition of C³I systems. In addition, Rome Laboratory's technology supports other AFSC Product Divisions, the Air Force user community, and other DOD and non-DOD agencies. Rome Laboratory maintains technical competence and research programs in areas including, but not limited to, communications, command and control, battle management, intelligence information processing, computational sciences and software producibility, wide area surveillance/sensors, signal processing, solid state sciences, photonics, electromagnetic technology, superconductivity, and electronic reliability/maintainability and testability.